TAMPEREEN TEKNILLINEN YLIOPISTO
TAMPERE UNIVERSITY OF TECHNOLOGY

EERO RÄISÄNEN

SIMULATION OF ASTROCYTE-NEURON NETWORKS

Master of Science Thesis

Examiner: Prof. Jari Hyttinen
Thesis Advisor: Dipl.-Inf.(FH) Kerstin Lenk
Examiner and Topic Approved in the Faculty of Natural Sciences Council Meeting 6th of July 2015

ABSTRACT

Eero Räisänen: Simulation of Astrocyte-Neuron Networks
Master of Science Thesis, 62 pages 2 Appendix pages
July 2015
Masters degree programme in Science and Engineering
Major: Biomeasurements
Examiner: Prof. Jari Hyttinen
Keywords: astrocyte, neuron, simulation, network, biology

The modern neuroscience aims for more and more detailed understanding of the reasons, which form the basis for search for cure or diseases related to the brain. Today we know that brain consists of multiple different cell types and functional organs ranging from blood vessels to glia cells and neurons. Each cell type has its specific functions which can be for example structural, immunological or signaling.

To study the functions of different living systems, it is often necessary to disturb the normal function to understand the underlying mechanisms. For this reason, methods for avoiding the use of model animals have been developed. One of the tools available for this is *in silico* modeling of the systems.

For this work, I have developed a computational model of a joint function of two cells types by combining existing models. Neurons form a neuronal network which is modeled using INEX by Kerstin Lenk (Lenk, 2011). The other cell type called astrocytes are modeled by Lallouette's UAR model (Lallouette, De Pittà, Ben-Jacob, & Berry, 2014) and a near synapse simulator interface together with De Pittá's presynapse model (De Pittà, Volman, Berry, & Ben-Jacob, 2011). The combined model is called INEXA. We present this simulation scheme in an attempt to model the interactions of astrocyte network and neuronal network.

Eighteen simulations were run to test different stages of the simulator. In phase one, the simulator INEX was run so that neurons had no synaptic strengths to get noise output of the basic activity driving the network. In phase two, Tsodyks-Markram presynapses were added to the neuronal network. In phase three, the presynapse area simulation including local astrocytes was added, and in phase four, the full INEXA was tested with 10%, 20% and 30% of the simulated culture being astrocytes.

The results show that the interconnected simulated astrocyte-neuron networks have properties that induce population bursting behavior while restricting hyperactivity. As such the astrocytes could be related to modulating signaling patterns towards bursting and restricting epileptic behavior.

TIIVISTELMÄ

Eero Räisänen: Simulation of Astrocyte-Neuron Networks
Diplomityö, 62 sivua, 2 liitesivua
Heinäkuu 2015
Biotekniikan diplomi-insinöörin tutkinto-ohjelma
Pääaine: Biomittaus
Tarkastaja: professori Jari Hyttinen

Nykyaikainen neurotiede pyrkii yhä tarkemmin ymmärtämään syitä, joiden pohjalta voidaan etsiä parannuskeinoja aivoihin liittyviin sairauksiin. Nykyään tiedämme, että aivot koostuvat useista eri solutyypeistä ja elimistä, joita ovat esimerkiksi verisuonet, glia-solut ja neuronit. Jokaisella solutyypilla on oma tehtävänsä, joka voi olla esimerkiksi rakenteellinen, immunologinen tai viestinvälitys.

Elävien systeemien tutkimisessa joudutaan usein rikkomaan mekanismin normaali toiminta, jotta mekanismin toimintaa voitaisiin ymmärtää. Tästä syystä jatkuvasti kehitetään metodeja välttää eläinmalleja. Yksi käytössä olevista työkaluista on systeemin mallinnus *in silico*.

Tätä työtä varten olen luonut laskennallisen mallin kahden solutyypin yhteistoiminnasta yhdistelemällä olemassa olevia malleja. Neuronit muodostavat neuroverkon, jotamallinnetaan Kerstin Lenk:in INEX mallilla (Lenk, 2011). Toista solutyyppia kutsutaan astrosyyteiksi ja niiden toimintaa mallinnetaan Lallouetten UAR mallin (Lallouette et al., 2014), synapsinläheisen astrosyyttimallin ja De Pittán presynapsimallin avulla (De Pittà et al., 2011). Yhdistettyä mallia kutsutaan nimellä INEXA. Pyrimme tällä simulaatiojärjestelmällä mallintamaan astrosyytti ja neuroverkkojen yhteistoimintaa.

Simulaattorin eri osien lisäämisen vaikutuksia testattiin kahdeksallatoista simulaatiolla. Ensimmäisessä vaiheessa neuroverkkoa ajettiin synapsien voimakkuudella nolla, jolloin saatiin näkyviin verkkoa ajavan perusaktiivisuuden aiheuttama kohina. Toisessa vaiheessa tutkittiin neuroverkon ja Tsodyks-Markram presynapsien vastetta kohinaan. Kolmannessa vaiheessa synapseihin liitettiin synapsinläheiset astrosyyttimallit ja neljännessä vaiheessa koko INEXA-mallia testattiin käyttämällä 10%, 20% ja 30% astrosyyttejä sisältäviä solumääriä simuloidussa viljelmissä.

Tulokset viittaavat siihen, että toisiinsa liitetyillä simuloiduilla astrosyytti-neuroverkoilla on ominaisuuksia, jotka tuottavat koko neuroverkon laajuisia purkauksia ja samalla vähentävät verkon yliaktiivisuutta. Täten astrosyyttien toiminta voisi liittyä neuronien viestinnän modulointiin kohti purkaustyyppistä toimintaa ja epileptisen toiminnan rajoittamiseen.

PREFACE

This thesis has been written based on my work as a research assistant at BioMediTech in Tampere during the last two years. It has been an honor to be part of Jari Hyttinen's Computational Biophysics and Imaging Group (CBIG).

I want to thank both Professor Hyttinen and my mentor, project researcher Kerstin Lenk for their continuous support and guidance in developing the model. I would also like to thank Hugues Berry and Jules Lallouette for many interesting conversations regarding astrocyte biology, and also for their contributions for the model. In addition, I want to thank all my co-workers at BioMediTech. It has been a great two years working with you all.

With this work I want to honor my grandfather Esko Räisänen, who passed away during my neuroscience studies at Glasgow University.

I have a special thanks for my family and friends for their support. In particular I would like to thank my girlfriend and my parents for keeping my feet on the ground and helping to concentrate on what is relevant. My brother has always been there to support and discuss about problems I have faced during these years. I've been inspired by my sister who stops at nothing and has forged her own path in the world.

Also I would like to thank in general everyone who has been there to talk, spend time and grow up with.

Tampere, 28.7.2015

Eero Räisänen

TABLE OF CONTENTS

LIST OF FIGURES

LIST OF ABBREVIATIONS

ADP	Adenosine disphosphate
AMPAR	α-amino-3-hydroxy-5-methyl-4-isoxazolepropionic acid receptor
ANN	Artificial neuronal network
ATP	Adenosine trisphosphate
CNS	Central nervous system
DFT	Discrete fourier transform
ER	Endoplasmic reticulum
FC	Fluorocitrate
fMRI	Functional magnetic resonance imaging
GABA	Gamma-amonibutyric acid
GFAP	Glial fibrillary protein
IP_3	Ionositol trisphosphate
MEA	Microelectrode array
mGluR	Metabotropic glutamate receptor
NMDAR	N-Methyl-D-Aspartate receptor
PIP_2	Phosphatidylinositol 4,5-bisphosphate
PPD	Paired pulse depression
PPF	Paired pulse facilitation
SNARE	Soluble NSF Attachment protein

1 INTRODUCTION

How the human brain works is one of the great mysteries of our time. The earliest recorded references to human brain are from 17th century BC in papyrus hieroglyphs (Feldman & Goodrich, 1999). The papyrus containing the markings describes symptoms, diagnosis and prognosis for two patients who were wounded in the head and had fractured skulls. The papyrus describes the symptoms in great detail while the lack of understanding the medical reasons behind the symptoms is apparent.

The modern neuroscience aims for more and more detailed understanding of the reasons, which form the basis for the search for cure or diseases related to the brain. Today, we know that the brain consists of multiple different cell types and functional organs ranging from blood vessels to glia cells and neurons. Each cell type has its specific functions which can be for example structural, immunological or signaling. The most famous signaling cell type is neuron. However, of the all cell types in a cortex, neurons correspond to 27–60% (Collins, Airey, Young, Leitch, & Kaas, 2010) . What is the purpose of the rest 40–73% of the cells?

Majority of the cerebral volume is taken by cells called glia cells. These cells perform multiple different important functions in the brain. Neuroglia are not one group but consist of multiple cell lines. Oligodendrocytes form myelin sheaths by wrapping around neuronal axons (Kiernan 2005, p. 20). This speeds up transmission along axons making the neurons able to transmit signals for long distances in shorter times (Kiernan 2005, pp. 22–23). Microglia may perform multiple tasks ranging from immunogenic supportive tasks like phagocytosis (Kiernan 2005, p. 33).

Neurons have been thought to form the basis for information processing in the brain. However, recently one glia cell type called astrocytes have been identified as a possible another cell type involved in information processing. The astrocytes are connected to neurons and to brain blood supply (Takano et al., 2006) as well as forming networks of their own (Halassa, Fellin, Takano, Dong, & Haydon, 2007). As such, they are ideally placed for local information processing. There have been studies (Bonansco et al., 2011; Lalo et al., 2014; Larrosa, Pastor, López-Aguado, & Herreras, 2006; Perea & Araque, 2007) where astrocytes have been studied for their individual effects. The final interpretation of their modulatory effect to neuronal network function is difficult and some of the results seem contradicting (López-Hidalgo & Schummers, 2014).

We approached the problem from a computational point of view and propose a simulation scheme, which describes different functions of astrocytes in mathematical formulas in

order to study the possible effects of astrocytes to neuronal network function. The simulation is based on previous work done by Kerstin Lenk on simulations of neuronal networks with INEX (Lenk, 2011).

There have been other models (Amiri, Bahrami, & Janahmadi, 2012; De Pittà et al., 2012; Gordleeva, Stasenko, Semyanov, Dityatev, & Kazantsev, 2012) describing the functionality of astrocytes at tripartite synapses, but so far there has not been a model, which comprises of all the aspects mentioned. This is the first model at this scale trying to grasp the functionality of neuron-astrocyte networks.

INEX describes neurons, which are connected to each other with synapses. A synapse is a connection between two neurons, where the cell membranes are brought almost to contact with each other. The first neuron called presynaptic neuron releases neurotransmitters into the small space left between the two cells when a spike occurs. This space is called synaptic cleft. The other neuron called postsynaptic neuron detects the transmitters and acts according to the transmitter in the cleft by increasing or decreasing the probability of the postsynaptic neuron also spiking.

Astrocytes form tripartite synapses where a synapse is wrapped by an astrocyte process. The neurotransmitter released by the presynaptic neuron is now also detected by the astrocyte. Astrocytes can monitor the information flow even from thousands of synapses. Astrocytes respond to the signals in the synapses with a calcium signal inside the cell. Based on these internal calcium signals, the astrocytes can also release transmitters back to neurons. These transmitters modulate the functionality of the synapses the astrocytes are connected to. We modeled this by a replica of an astrocyte interface simulator by De Pittá et al. (De Pittà et al., 2011), which is based on Tsodyks-Markram synapse simulation. The small internal calcium signals caused by the releases at the synapses can spread to the whole astrocyte. Also astrocytes are connected to each other through gap junctions. This allows the calcium signals to spread between astrocytes. To simulate this, we used the UAR simulator by Lallouette et al. (Lallouette et al., 2014). However, so far there has been no models to show the combined effect of these functions in neuronal network level. The purpose was to study how astrocytes could affect the neuronal network behavior and suggest a greater role for astrocytes in neural computation than previously thought. Our hypothesis of the interconnected astrocyte-neuron network function is that it induces bursting behavior while restricting hyperactivity.

We aim to study the effects of astrocytes *in silico*. Later it would also allow us to explore the key changes in the communication in interconnected computational systems formed by astrocyte and neuronal networks in order to identify the mechanisms to be targeted with drugs. Also understanding the computation performed by different cells might eventually bring us closer to understanding our own thoughts, minds, and self.

2 THEORETICAL BACKGROUND

In this section, we will discuss first about the biology relevant to the simulation starting from basics and building up. After that, we discuss shortly about the simulations made by others describing the biological phenomena. The section biology will consist of basic cell communication regimes, relevant transmitter molecules, receptors and cell types. At first, we will start with the cell communication.

2.1 Biology

Essential difference between single and multicellular organisms is not only the size but also the complexity. Since in multicellular organisms a single cell is an autonomous functional unit working together with other autonomous units to form something bigger than the sum of their parts, some form of communication is needed to keep the cells working together. Cells communicate through multiple channels which have been defined as endocrine, paracrine, neuronal and contact dependent signaling between cells (Alberts et al. 2009, p. 533). Endocrinal communication involves hormones. These messenger molecules are spread by injecting them into the blood stream by various cells. The target of hormones is not a single cell but rather all cells the hormone reaches. In paracrine messaging, the message effect is meant for a smaller group of cells. The messenger molecule is released into extracellular matrix where it only spreads smaller distances. For even more specific communication cells can use contact dependent signaling or neuronal synapse based messaging. For our purposes paracrine, contact based and neuronal signaling methods are the most important ones.

In the following sections, we will discuss the most important signaling pathways and transmitter molecules forming the basis of neuronal and astrocyte communication in the pathways used in the simulation.

2.1.1 Cell membrane, action potential and MEA

Each cell has an inside called cytosol or intracellular space and an outside called extracellular space. These two spaces are divided by a lipid bilayer forming a two dimensional liquid or membrane, which lets through water and other small molecules, but through which large water soluble molecules and ions do not pass so well (Alberts et al. 2009 p. 389). The membrane has large amounts of membrane proteins bound to it. Some of these proteins form complexes, in which multiple proteins have joined together to perform a specific function. The function can be catalyzing a reaction or forming a physical opening through the membrane for other molecules to move through it (Alberts et al. 2009, pp. 372–375).

Some of these openings let through ions and are called ion channels. The ion channels let through charged molecules (Alberts et al. 2009, pp 400–405). Since the membrane does let through ions, the permittivity of the membrane to that ion is determined by the number and permittivity of the sum of open channels letting through the ion at any given moment.

Membrane voltage

There are two driving forces for ions across the membrane (Alberts et al. 2009, p. 392). First is the concentration of the molecule at each side of the membrane. The ions will diffuse through the membrane faster from the higher concentration to the lower than the opposite. The concentration of the ion is ion specific and thus different ions can have different and even opposing ion concentration gradients through the membrane.

Ion concentration across a membrane is technically an electric current and the permittivity of the membrane determines the resistance of the membrane. Since the ions are charged, they will form a voltage across the membrane when they have moved to the other side. The accumulation of charges at the lower concentration side forms a voltage gradient across the membrane. Since the ions are charged, the voltage formed will have an effect to the current through the membrane. Eventually the current stops when the voltage over the membrane resistance raises high enough to exactly oppose the ionic flux driven by the concentration gradient.

When only one ion is taken into consideration, this dependency of membrane voltage of concentration difference is described by Nernst equation (Bear et al. 2007, p. 65):

$$1)\ V = \frac{RT}{zF} ln \frac{[i_{out}]}{[i_{in}]}$$

In the equation, V is the membrane voltage at equilibrium, R the ideal gas constant, F Faraday's constant, z is the charge of the ion and [i] the ion concentration.

However, this is the case only for a single ion. Since concentration gradient is unique for each ion that part will stay the same for each ion, but voltage difference formed by contribution of different ions is the same. The membrane can have only one voltage. To calculate the membrane potential of a cell membrane when multiple ions contribute, the Goldman equation is being used. The main difference between the Nernst equation and Goldman equation is that the Nernst equation does not depend on permeability. Eventually the membrane will be at equilibrium as long as there is any permeability on the membrane. However, when there are multiple different ions contributing to the membrane potential, the speed of diffusion of different ions becomes important. Goldman equation (Matthews 2007, appendix B) is similar to the Nernst equation with the exception of permeability terms.

$$2)\ V = \frac{RT}{F} ln \left(\frac{\sum P_{M_i^+} [M_i^+]_{out} + \sum P_{A_j^-} [A_j^-]_{in}}{\sum P_{M_i^+} [M_i^+]_{in} + \sum P_{A_j^-} [A_j^-]_{out}} \right)$$

In Goldman equation (equation 2), the R, T an F are the same as in Nernst equation. Within the natural logarithms there are differences. First of all, each concentration [] is multiplied by their respective permeability P to that ion. Also the negative and positive charges induce opposing voltages and as such the in- and the out-terms for those ions are at the opposing sides of the division. Now, we have a final voltage over the membrane which changes relative to permeability of each ion.

Neurons communicate using the membrane voltage as carrier to the signal (Bear et al. 2007, p.76). This is why they are called electrically active cells. They use their membrane voltage to carry a signal over large distances.

Action potential

As in the last section was discussed, the membrane potential depends on permeability of the cell membrane to ions together with concentration gradient of the ions. Since the voltage drives ions to the opposing direction as the flux of ions from concentration gradient, the concentrations do not change by much. The balance of ion concentrations is also maintained by ion pumps transporting ions through the membrane.

The normal resting potential of a neuronal membrane is around -65mV (Bear et al. 2007, p. 62). This is mainly due to sodium and potassium concentrations and permeability of the membrane to the ions (Bear et al. 2007, p. 67). The membrane potential may be changed by opening or closing ion channels and thus by changing the permeability of the membrane. The changes are local and gates opening at a certain area will have an effect to the voltage only at certain distance away from the gate. Neurons have a tree like structure which collects signals from other neurons (Bear et al. 2007, pp. 41–42). Those signals alter the membrane potential of the neuron at an area called axon hillock to determine if a new action potential is fired (Bear et al. 2007, p. 97). If the membrane potential is brought closer to 0V, it is said to be depolarized. On the other hand, permeability changes causing the membrane potential to drop lower than the resting potential is said to hyperpolarize the membrane.

The axon hillock is a part of the neuron, where the inputs of various synapses are integrated. If the hillock is depolarized over a potential called action potential threshold, the membrane gets increasingly polarized. This is caused by voltage gated sodium channels, which as their name suggest open at a certain voltage. This means that the channels are closed when the membrane is at resting voltage and open when the membrane is depolarized enough. Action potential threshold is determined by the voltage opening enough voltage gated channels that it opens other nearby channels so that they again open other channels nearby them. This opening of channels along the membrane

transports the depolarization wave along an axon. Voltage gated potassium channels open at a small delay to bring the voltage back down as quickly as possible.

Measuring the action potential: Microelectrode array recordings

Microelectrode arrays (MEAs) are used to detect electrical changes at the membranes. The measurement setup consists of an array of micro sized electrodes, which record voltage changes in comparison to a reference electrode. The array measures local changes in voltages in a culture. Thus, the arrays can be used to study any electrically active cells. A MEA consists of an array of very small electrodes and the potential of the electrode is then compared with a reference electrode.

MEAs have been used for example to study human embryonic stem cell derived neuronal networks (Heikkilä et al., 2009). This allows for more ethical research than use of test animals. For example, neurotoxic testing can be performed on MEA cultured neuronal networks (Johnstone et al., 2010).

While neurons are electrically active cells the astrocytes are not. They do have membrane potential and even have voltage gated channels, but they are not used for signal transmission as the neurons do. Because of this MEA cannot detect astrocyte signaling. However, since neurons and astrocytes communicate with each other the neuronal signaling should change if astrocytes are present.

The INEX simulator has been used to simulate the behavior of growing neuronal networks on MEA plates and the simulator built for this work is built on top of the INEX. It has been used for example for simulation of developing human neuronal networks.

2.1.2 Endoplasmic reticulum and calcium signaling

In many cells that may or may not be electrically active, there is another important signaling pathway. This pathway involves a cell organelle called endoplasmic reticulum (ER). The ER is another membrane sack inside the cell. It contains a high concentration of calcium which can be released into the cytosol (Perea & Araque, 2005). The release of calcium occurs when a transmitter called ionositoltrisphophate (IP_3) opens gates at the membrane. Such gates are also found at the outer membrane and each type responds to different transmitter molecules.

In order to open the IP_3 gated channels at the ER, the IP_3 needs to be produced. This is done by catalyzing a reaction where IP_3 is formed. Catalysis of the reaction is done by a protein called phospholipase C (Gordleeva et al., 2012). This protein is activated when another transmitter is detected in the extracellular space by membrane proteins of the outer membrane. Thus, the signaling cascade of IP_3 begins outside the cell and ends up releasing calcium from internal storage of ER inside the cell (Bear et al., 2007, p. 162). Calcium can perform many different functions in the cell. For example in heart and

muscle, it causes the contraction of the muscle cell (Alberts et al., 2009, pp. 599–604). The cells signaling with calcium often have specific types of membrane proteins called connexins forming channels called gap junctions through two outer cell membranes and allowing diffusion of calcium and other molecules from one cell to another. This allows, for example, coordinated contraction of the heart. Also there is a subtype of neurons that form so called electrical synapses, where instead of chemical synapse a gap junction is formed to conduct the membrane potential of the first neuron to the next (Bear et al., 2007, pp. 103-105). However, it is different than chemical synapse, because it allows membrane potential information to flow both directions in the synapse in contrast to presynapse to postsynapse direction in chemical synapses.

Calcium waves, where the calcium signal spreads from one cell to another can be found in many parts of our body doing different tasks. However, since they do not involve voltage changes, they cannot be detected with an electrode. To detect changes in calcium concentration another method has to be used. One method is to use fluorescent markers and fluorescence microscope (Földes-Papp, Demel, & Tilz, 2003; Paredes, Etzler, Watts, Zheng, & Lechleiter, 2008). This method called calcium imaging can reveal the calcium signaling occurring at the cellular or even subcellular level. However, the higher resolution images are taken, the more time it takes. Thus, taking images that have sufficient temporal resolution for detecting calcium signaling usually means too low spatial resolution for detecting small scale events.

2.1.3 Relevant receptors and transmitters

There are multiple extracellular transmitter molecules, which are important for the pathways being modeled. Each of these transmitters is tied to at least one signaling cascade. We will start with the most common transmitter called glutamate. Each of these molecules or keys have receptor molecules or locks into which each of them fits. The receptor can respond to some similar molecules as well but usually they respond the specific transmitter molecule the strongest.

Glutamate

Glutamate is an amino acid which is an excitatory neurotransmitter. This means that introduction of glutamate to synaptic cleft opens sodium permeable gates, which have glutamate as ligand. These receptors include α-amino-3-hydroxy-5-methyl-4-isoxazolepropionic acid (AMPAR) and N-Methyl-D-aspartate (NMDAR) receptors. Both AMPAR and NMDAR let through both sodium and potassium and have equilibrium potential near 0V (Bear et al., 2007, pp.154–155). Thus, if glutamate is introduced, the membrane at the synapse area is depolarized. The summation of depolarization from multiple synapses at the axon hillock can cause the neuron to fire an action potential.

Glutamate is also detected by another type of receptor at the astrocytes. If an astrocyte detects glutamate through metabotropic glutamate receptors (mGluR) it initiates catalysis for IP3 production and thus contributes to release of calcium from internal storage.

Neurons can also have mGluR and NMDAR at the presynapse areas. These extrasynaptic glutamate receptors alter the release of neurotransmitters at the synapses. Introduction of glutamate to the receptors potentiates the synapse (Perea & Araque, 2007).

GABA

γ-Aminobutyric acid (GABA) is the main inhibitory transmitter in the brain (Bear et al., 2007, pp.146–147). It can act on ligand activated gates or metabotropic receptors, which open channels by a secondary messenger molecules (Bear et al., 2007, pp.157–158). However, the function of both types of channels is to hyperpolarize the membrane. When the membrane is hyperpolarized more or stronger excitatory voltages are required for action potential initiation.

While glutamate and glycine are synthesized from glucose and other precursors, the precursor for GABA is glutamate. Thus, by introducing only one enzyme called glutamic acid decarboxylase the major excitatory neurotransmitter is converted into major inhibitory transmitter (Bear et al., 2007, p. 147, p.164).

ATP and adenosine

Adenosine trisphosphate (ATP) is the main energy storage molecule in cells. However, it and its derivatives adenosine disphopshate (ADP) and adenosine are also used as transmitter molecules. ATP released by astrocytes can act on multiple different receptor types some of which are potentiating and some depressing synaptic output. Adenosine acts primarily on depressing A1 receptors. ATP is hydrolyzed into ADP and adenosine after exocytosis.

The functions of ATP signaling by astrocytes is not entirely clear (Lalo et al., 2014). However, it has been suggested that ATP release is another pathway for transmitting calcium waves from one astrocyte to another. It has been shown that adenosine accumulating in the brain is responsible for sleep pressure (McIver, Faideau, & Haydon, 2013).

2.1.4 Cell types

The communication between neurons and astrocytes form a computational machinery that includes memory and plasticity. Neurons transmit signals through synapses and astrocytes monitor synaptic transmission. This allows for two complex systems to interact in ways that are not completely understood. In the next chapters we will look more closely into the functionality of these cell types.

Neurons

As explained before neurons transmit signals using membrane voltage. Neurons can be of many shapes and sizes. Commonly a neuron has soma, which is the center of the cell containing nucleus and other organelles. Usually a neuron has a dendritic tree which receives incoming synapses and an axon, which transmits signals forwards to next cells (Bear et al., 2007, pp 29–45).

The interface between two neurons is a synapse. In a chemical synapse, the signal is changed from electrical signal transmitted at the membrane to chemical signal. The type of the chemical species called neurotransmitter determines the effect of the signal to the next neuron. Each neuron may have hundreds or even thousands of synapses. However, they are all the same type.(Bear et al., 2007, pp. 133–167) So a neuron may release transmitters that increase the probability of the next neurons spiking or inhibit them. Based on this, the neurons can be categorized into two main types. The first type is excitatory and the second is inhibitory neuron. The most abundant excitatory neuron type releases glutamate and the inhibitory neuron type GABA. These same substances are also released by astrocytes into extracellular space as gliotransmitters (Angulo, Le Meur, Kozlov, Charpak, & Audinat, 2008; Perea & Araque, 2005).

The membrane machinery transmitting signals is similar for all neuronal types. It can be either as it was described earlier, that the membrane potential is moved along the axon by opening voltage gated channels, which open the next ones, or the moving of voltage can be helped by a type of glia cell called oligodendrocyte. Oligodendrocyte wraps around the axon at certain intervals and alters the transmission into saltatory conduction in which voltage difference jumps over the high resistance areas into the next area free of oligodendrocytes myelin (Kiernan, 2005, pp. 20–22). This increases the speed of conduction.

At the synaptic terminal where the action potential is changed from membrane voltage difference to neurotransmitter release, it is done using voltage gated calcium channels. While the conduction use voltage gated sodium channels the voltage difference at the nerve terminal is converted into calcium influx. This calcium binds to a soluble NSF attachment protein receptor (SNARE). When calcium binds to this protein it fuses transmitter containing vesicles with the membrane of the terminal, releasing its contents into the synaptic cleft (Bear et al., 2007, p. 116). New vesicles are formed and docked with SNARE proteins to replenish the synapse for next action potential.

Each neuron is releasing only certain types of transmitters. Even though it is known that a neuron can co-release different transmitters they are generally having either inhibitory or excitatory effect (Bear et al., 2007, 141–142). Thus, all synapses from a single neuron will have the same effect to the neurons they are connected to. For example, glutamatergic neurons are excitatory neurons and promote firing of action potential in the next neuron.

Glia cells and Astrocytes

Neuroglia are a diverse group of cells that are not neurons found in abundance in the brain. They are known to perform many different tasks in the brain from nourishing neurons to maintenance of chemical balance to immunogenic response (Kiernan, 2005, pp. 30-33). One group of cells in particular is very interesting since it is known to do all these tasks and possibly more. The cell type in question is astrocyte. These star shaped cells were originally thought to offer structural and chemical support to neurons and their gap junctions joining their cytosols were thought to be for quick distribution of excess ions away from the area where neurons were highly active (Kiernan, 2005, pp. 31–32). Especially maintaining potassium balance was considered to be their main task.

Astrocytes are also known to form a part of a vital component in our brain called blood brain barrier (Abbott, Patabendige, Dolman, Yusof, & Begley, 2010). This is a layer of cells which filters nourishments and ions from blood stream so that the rest of the brain is never directly in contact with the blood supply. Blood brain barrier is a vital defensive and chemical balance structure since it prevents access from pathogens to the brain as well as maintains different extracellular chemical balance in the brain than is found in the other parts of the body.

In case of damage to central nervous system (CNS), a structure is formed into the damaged area and this scaring comprises mainly of astrocytes (Sofroniew, 2005). The scaring is the first step in healing of CNS. However, in some cases the scarring formed by astrocytes can be detrimental to clinical outcome. This is particularly troublesome with some *in vivo* long term electrical measurements since the scaring encapsulates the electrodes and makes them virtually useless (Polikov, Tresco, & Reichert, 2005).

The astrocytes just like neurons come in at least two different types (Kiernan, 2005, p. 32). They can be distinguished by their chemical composition. Fibrous astrocytes contain Glial fibrillary acidic protein (GFAP) which is an intermediate filament. These proteins allow for more rigid structures. The fibrous astrocytes are found mainly in the grey matter, which essentially means that these are the type found near neurons cell bodies. Astrocytes which lack this protein are called protoplasmic astrocytes and are mainly found in the white matter. White matter consists mainly of neuronal axons and oligodendrocytes wrapped around them. Tightly packed lipid membranes, which are essentially fatty acids, give the tissue its white color. The astrocytes we are interested in are the fibrous astrocytes. It is also possible that these astrocytes divide into subgroups but that is not known.

While oligodendrocytes wrap their processes around axons to speed up the information transfer, the astrocytes wrap their processes around synapses (Kiernan, 2005, p. 32). This allows them to detect transmitters leaking from the synapse (Porter & McCarthy, 1996). Astrocytes are known to take up transmitters like glutamate, but they also respond to the synaptic input with increased calcium through mGluR activation at the astrocyte process.

An astrocyte may have wrapped around up to thousands of synapses (Hines & Haydon, 2014); yet every synapse is connected up to one astrocyte. This places astrocytes into unique position in sensing the general activity of the neuronal network since they have a large sample from multiple synapses. Astrocytes can also modify synaptic transmission at single synapse level.

As mentioned, the astrocytes are also in direct contact with the blood vessels in the brain (Takano et al., 2006). Functional magnetic resonance imaging (fMRI) is used to image neuronal activity indirectly. This means that it does not actually image neuronal activity but it detects increased blood flow through areas in which activity occurs (Jueptner & Weiller, 1995). Thus, there is a mechanism for increasing blood flow in relation to neuronal activity. This would suggest that astrocytes are also involved in regulating blood supply related to neuronal activity detected by fMRI.

2.1.5 Communication differences between astrocytes and neurons

As we have seen so far, the neurons and astrocytes utilize different mechanisms for transmitting and integrating information. However, in the end it all comes down to membranes and concentration gradients and voltages across those membranes. In the next sections we will look into the cellular structures responsible for the differences and how they are linked together.

Calcium and voltage

Calcium is used in many cells as a messenger molecule. Astrocytes use it to integrate signals, muscle cells to contract, and neurons to release transmitters. Calcium signaling can be based on concentration gradient across the outer membrane as in nerve terminals or stored inside the cell in another membrane. The main difference is that while the calcium moving through the ER membrane within the cell does not induce voltage to the outer membrane of the cell the voltage of the outer membrane is the key to opening the voltage gated channels at the nerve terminal. In the case of the nerve terminal, also calcium ions need to be taken into account when calculating the membrane potential with Goldman equation. However, when calcium is released from within the cell from ER to another compartment inside the cell, no net charge is moved across the outer membrane and no voltage at the outer membrane is involved. Astrocytes exhibit two types of calcium signaling. There are local calcium events occurring at astrocyte processes and full astrocyte wide calcium signals (De Pittà et al., 2012).

The ER is the main structure at astrocytes involved in calcium signaling. Signaling cascades involving calcium use some pathway to open calcium permeable gates at the ER membrane to increase calcium concentration in the cytosol. The ER in astrocytes is separated into small spatially distinct compartments as functionally distinct units. This allows the calcium signals to be spatially and temporally restricted within the cell (Golovina, 1997). Neurons have the ER membrane as well. However the calcium used

for release of neurotransmitters is thought to originate from extracellular space and enter the synapse through voltage gated calcium channels (Llinás, Steinberg, & Walton, 1981). This means that there is a higher concentration of calcium outside the cell than inside and the concentration and voltage gradients drive calcium into the cell when permeability increases.

Time and spatial scales

The temporal and spatial properties of these events are also of importance. The different opposing signals start to make sense when they are put to their respective time scales. Astrocytes have two forms of calcium signaling. One is spatially restricted within the processes of the astrocytes or full astrocyte wide signaling that can spread in the astrocyte network (Kozlov, Angulo, Audinat, & Charpak, 2006).

The spatial scales of the full astrocyte signaling is in seconds timescale (Lallouette et al., 2014) while the spatially restricted calcium signals occur in the timescales of hundreds of milliseconds (Winship, Plaa, & Murphy, 2007). The calcium waves or "glissandi" are blocked by tetrodotoxin, which inhibits neuronal signal transmission (McIver et al., 2013). This indicates that the calcium waves occurring in astrocyte network level are driven by neuronal activity. Astrocytes occupy spatial domains that are approximately 100µm in diameter. The astrocytes control their own space (Bushong, Martone, Jones, & Ellisman, 2002). In the same study it was also noticed that presence of blood vessels influence interastrocytic interactions. The astrocytes seemed to be competing for access to a passing blood vessel.

While astrocytes function in the timescales of hundreds of milliseconds to seconds, neurons transmit signals in millisecond scale. An action potential at the membrane lasts approximately 2ms (Bear et al., 2007, p. 76). The transmission speed of a typical axon is in the scale of 10m/s (Bear et al., 2007, p. 94).

2.2 Models

Modeling is a useful tool for testing theories and trying to understand complex problems and when the model is good enough it can produce predictive results. Predictive models can test theories and produce results of possible changes in the system in small amount of time compared to biological research done in a lab.

A model has its own abstraction level. This means that it will assume certain things and make approximations. No model is perfect and knowing the limitations of a model is important. The models used for building this combined model are phenomenological meaning that they describe the phenomena rather than try to be perfectly accurate. This allows for more freedom and building a model of more complex systems than an accurate model would. There will be a tradeoff between accuracy and computing power requirement.

In the next chapters we will go through the three models used to build the neuron-astrocyte model INEXA and few other models describing tripartite synapses.

2.2.1 INEX model by Kerstin Lenk

INEX is a phenomenological model built to simulate neuronal firing in a MEA culture (Lenk, 2011). It is a cellular automaton in which inhibitory and excitatory neurons are connected to each other with synapses and a general noise is applied. Each neuron has its own base probability of generating spikes and this is driving the network activity. The input from each spiking neuron connected to a neuron via a synapse effects the probability of a spike being generated at the next neuron. The part of the biology being covered by INEX includes neuronal dendrites, axons, synapses, and axon hillock computation.

INEX has been used for simulations of networks cultured on MEA plates for neuron amounts ranging from 100 to 10000 neurons (Lenk & Priwitzer, 2011; Lenk, 2011). The model works well for simulating spiking activity of MEA.

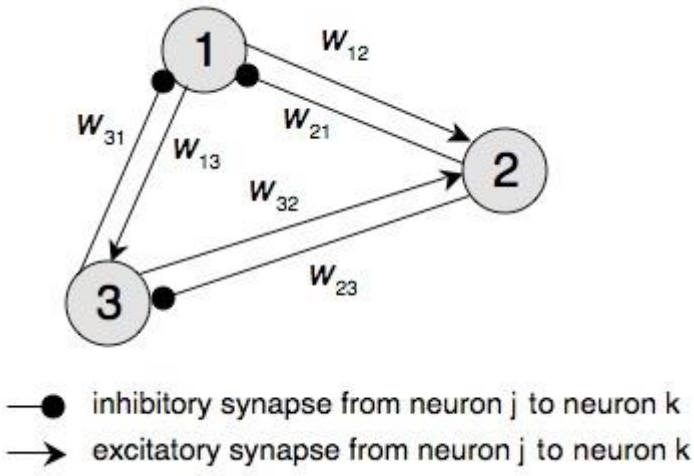

Figure 1: An example of a simulated neuronal network with two three neurons. Figure from (Lenk, 2011)***.***

Briefly, the INEX model is a cellular automaton whose cells are neurons with two possible states: ON or OFF. Each neuron obtains several inputs and produces exactly one output (spike or no spike). In order to simulate spontaneous activity, we assumed that the spikes obey an inhomogeneous Poisson distribution. The momentary firing rate λ_i of neuron i in time slice t_k was calculated as follows:

$$3)\ \boldsymbol{\lambda_i(t_k)} = \begin{cases} \boldsymbol{c_i + \sum_j y_{ij} \cdot s_j(t_{k-1})}, & \boldsymbol{if\ c_i + \sum_j y_{ij} \cdot s_j(t_{k-1}) > 0} \\ \boldsymbol{0}, & \boldsymbol{otherwise} \end{cases},$$

where c_i denotes the basic activity, y_{ji} the synaptic strength of all neurons j connected to neuron i and s_j the particular spike of the previous time slice of neuron j (1 for a spike and

0 for no spike). The parameter values were randomly chosen from a triangular distribution. The values lie between zero and an upper boundary that is at most 1 to indicate the release of all vesicles from the synapse. For c_i, the upper boundary varies from 0.01 to 0.03 with intervals of 0.01 to produce networks with different noise levels. For the excitatory synaptic strength y^+_{ji} boundary of 0.7 was used and for the inhibitory synaptic strength y^-_{ji} = -0.7.

The probability P_i for the occurrence of a spike in time slice Δt is defined as follows:

$$4)\ \boldsymbol{P_i(1\ spike\ in\ \Delta t)} = \boldsymbol{e^{-\lambda_i \Delta t} \cdot \lambda_i \Delta t}$$

The time slice Δt is chosen with a length of 5 milliseconds to cover the temporal length of the action potential and the subsequent refractory period. For each time slice, the algorithm tested if $x_i < P_i$, where x are uniformly distributed random values.

INEX also contains a spike time history variable f, which makes it more likely for a neuron to spike if there was a spike in the network in the previous time slice.

2.2.2 Presynapse model by De Pittá et al.

De Pittá et al. have introduced a simulation scheme for astrocyte-neuron communication at tripartite synapses. They introduced the model and its effects in a paper called "A tale of two stories: astrocyte regulation of synaptic depression and facilitation" (De Pittà et al., 2011) and later discuss the plausibility of the signaling pathway in the review article "Computational quest for understanding the role of astrocyte signaling in synaptic transmission and plasticity" (De Pittà et al., 2012).

The model uses Tsodyks-Markram (Tsodyks & Markram, 1997) synapse simulation together with an astrocyte interface. The astroycte is modeled with similar dynamics as a synapse, which responds to glutamate released to synaptic cleft. They have also modeled astrocytes with more complex functions previously to study calcium signaling in astrocytes in response to neurotransmitter glutamate (Wallach et al., 2014). The system being modeled is part of the scheme shown in Figure 2.

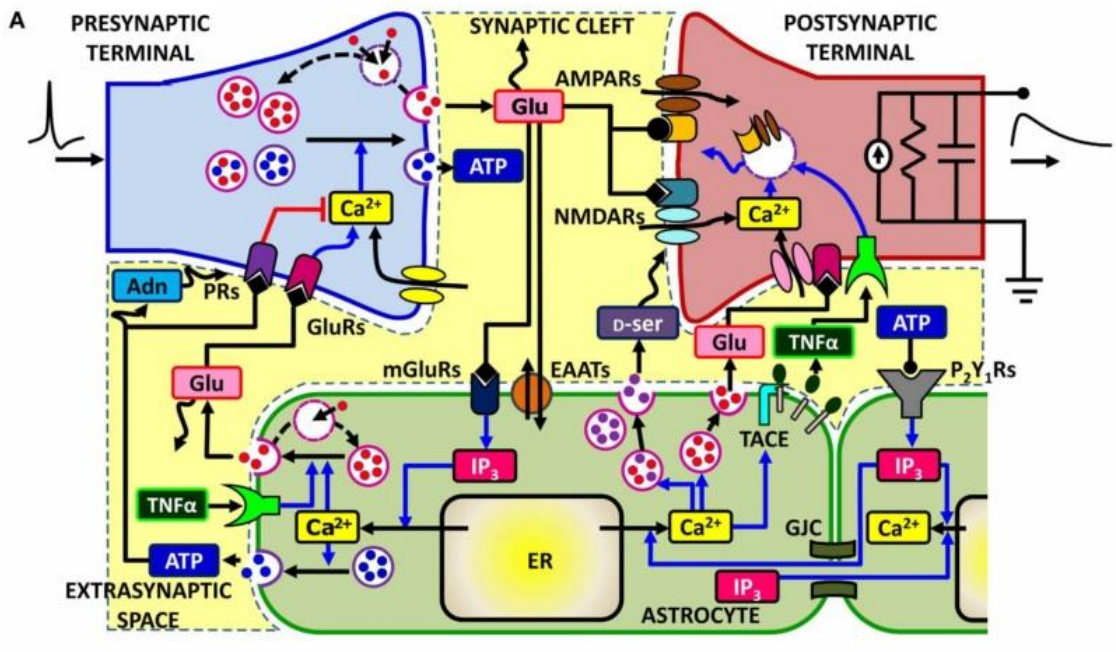

Figure 2: Pathways of astrocyte function by De Pittá et al. The model they used comprises of presynapse calcium dynamics, astrocyte dynamics and interfaces for detecting glutamate and releasing gliotransmitters to extrasynaptic space. Figure from (De Pittà et al., 2012)

Their results in De Pittà et al. (2011) show that a synapse can change between paired pulse depressing (PPD) and paired pulse facilitating (PPF) modes based on the gliotransmission and the total effect of receptors detecting the gliotransmission in extrasynaptic space. PPF means that when after a spike another spike occurs in a short interval, the next one will be stronger than the first one. On the contrary in PPD the second spike will be weaker. The change between the modes depends on the original release amount the synapse would have as well as the effect the presynaptic receptors have.

2.2.3 Chl and UAR models by Lallouette et al.

Lallouette et al. studied the spreading of calcium waves using networks of astrocytes comprising of 1331 astrocytes (Lallouette et al., 2014). This allows them to be set into a grid of 11x11x11 astrocytes in three dimensional space. Their Chl model uses differential equations to solve calcium signaling based on knowledge of those pathways. They then combine astrocytes having their own states with fluxes of IP_3 through gap junctions. Their results show that on the contrary to neuronal network, the more connected the astrocytes are the worse they transmit signals. In Figure 3 can be seen the calcium wave spread in differently connected networks as shown by the Chl model.

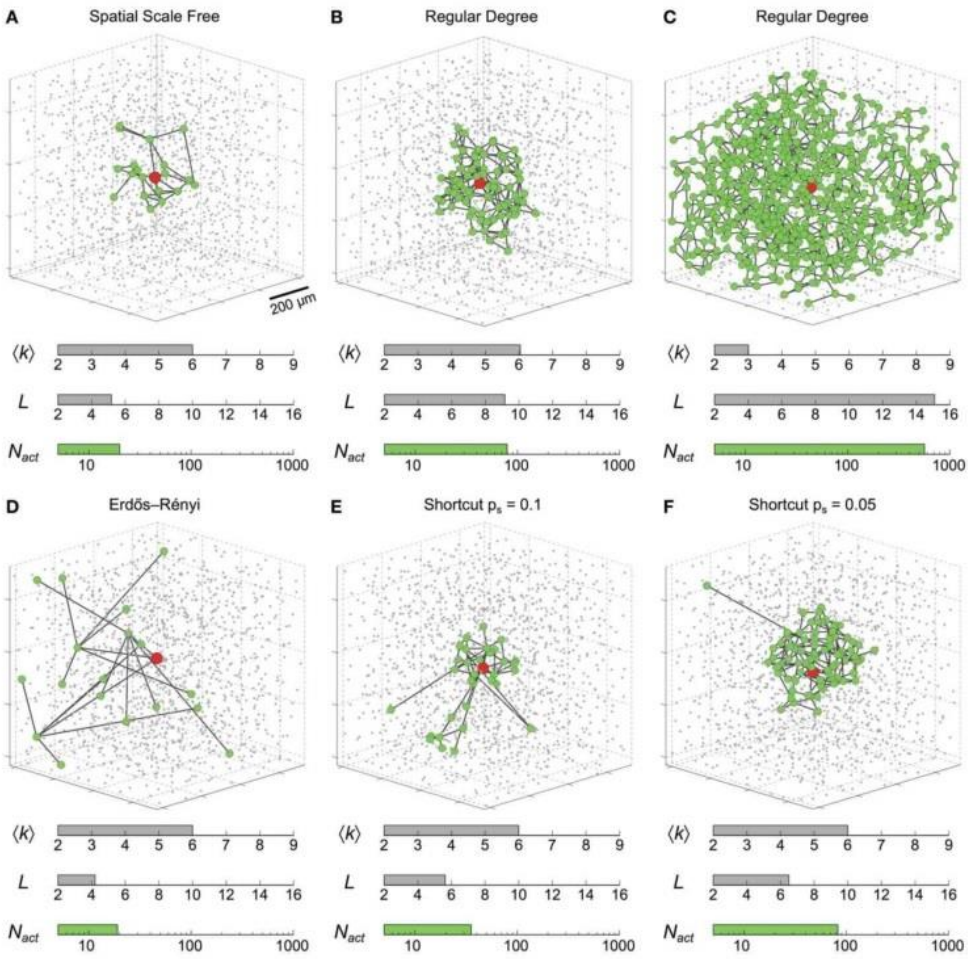

Figure 3: Six differently connected astrocyte networks being stimulated at the middle. Green dots show astrocytes activated during the simulation. Figure from (Lallouette et al., 2014)

Based on the results with the model using differential equations, they made a hypothesis of the spread of the wave to be related to two-hop-neighborhood of the astrocyte network. This means that each astrocyte transmitting signal to the next one has the IP_3 flux divided between its inactive neighbors but also the activation of the next astrocyte is related to the number of inactive neighbors. Thus, astrocytes two hops away will affect the effect of a flux induced by the first one. To test their hypothesis, they constructed a simplified model called UAR that takes into account these phenomena. The result indicates that the hypothesis is true. The UAR model uses three state astrocytes, probabilistic activation of astrocytes and fluxes between astrocytes. The conversion from Chl model to UAR model is illustrated in Figure 4.

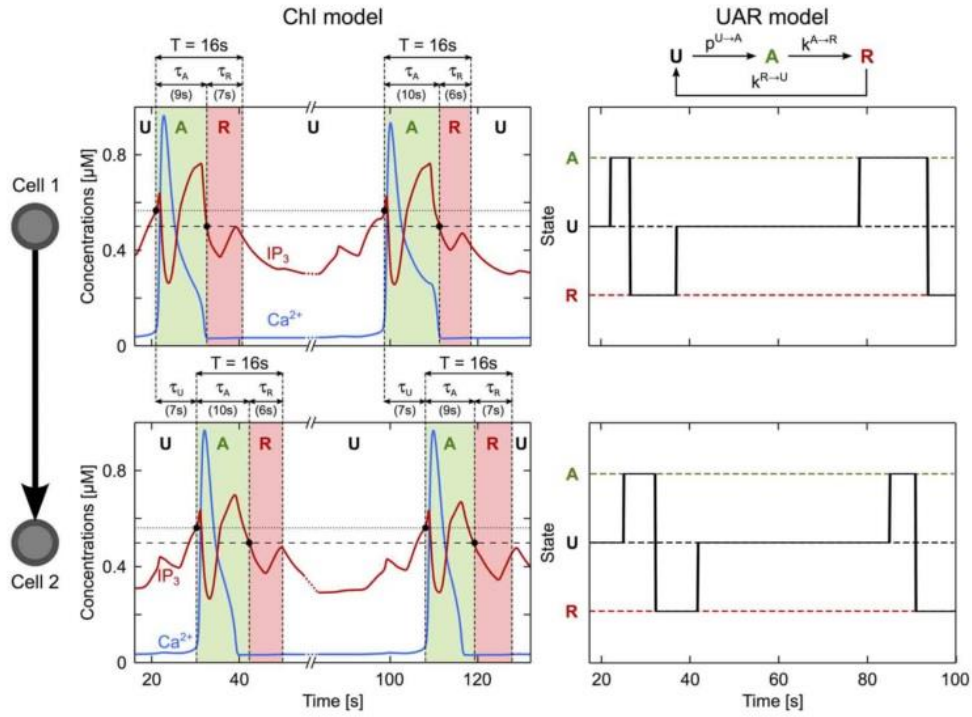

Figure 4: Conversion of Chl model using differential equations for accurate results to simplified UAR model. Figure from paper by Lallouette et al. (Lallouette et al., 2014)

The UAR model astrocytes can have three possible states: active signaling state (A), inactive dormant state (U) and refractory period (R) during which the cell cannot transmit calcium signal (Lallouette et al., 2014). At any time, the cell will be in one of these states and can transit between the active to refractory and back to inactive on its own depending on probability values based on average time the cell spends in these states. The astrocyte calcium signaling is governed by the following equations (Lallouette et al., 2014):

$$5)\ flux_{a\ out}(t_k) = \begin{cases} A: \frac{1}{I_a(t_k)} \\ U, R: 0 \end{cases}$$

$$6)\ flux_{a\ in}(t_k) = \sum flux_{b\ out}(t_k)$$

$$7)\ acv_a(c_a) = yc_a + b$$

$$8)\ P(U \to A)_a(t_k) = \begin{cases} flux_{a\ in}(t_k) > acv_a(c_a): \Delta t / A_{time} \\ flux_{a\ in}(t_k) < acv_a(c_a): 0 \end{cases}$$

$$9)\ P(A \to R) = \Delta t / R_{time}$$

$$10)\ P(R \to U) = \Delta t / U_{time}$$

Equation 5 describes the IP_3 flux out of the astrocyte to its neighbors when it was active. The flux is equal to 1 divided by the number of inactive neighbors. The fluxes into an astrocyte were summed up in equation 6.

The flux in must be higher than a threshold set for the activation of the astrocyte. This threshold was set with the linear equation 7. In the equation, y is the increase of needed flux per each additional connection c_a and b is the baseline threshold.

Equations 8-10 describe the probabilities of state change. The state changes from activated to refractory and from refractory to inactivated state which happens spontaneously over time. The probability for activation is based on the fluxes being higher than the threshold.

2.2.4 Other models

In this section, we go through a few other results obtained with astrocytes *in silico*. We discuss two other models and one neuronal network classification problem using astrocyte effects as part of an artificial neuronal network (ANN). While the previous three (see section 2.2.1 to 2.2.3) will be used for building the astrocyte model, these three are purely for comparison.

Tripartite synapse simulation by Gordleeva et al.

In this model, Gordleeva et al. (2012) show that activations of local astrocytes may effectively control network through the combination of different actions of gliotransmitters. Their model consists of a computational model of synapses involved in spontaneous firing of neuronal network using a mean field approach. The output of the neuron is channeled back as output through the mean field of a neuronal network. Thus, the neuron will have an effect to the neuronal network and the network affects the firing pattern of the synapse. In their model, they use glutamate as a transmitter to depress presynaptic output and D-serine to increase postsynaptic response. The simulation scheme can be seen from Figure 5.

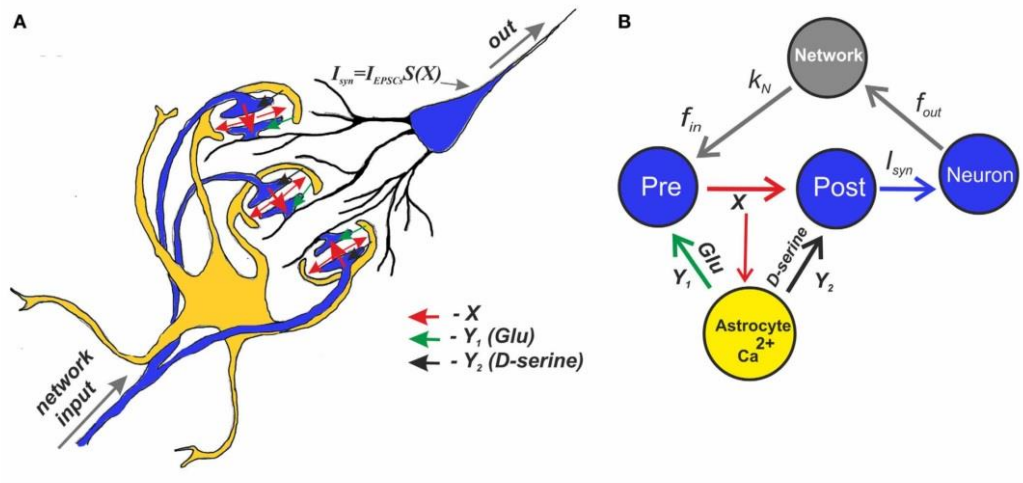

Figure 5: Simulation scheme by Gordleeva et al. The input of the neuron to presynapse is calculated from a mean field of network input. Astrocyte gliotransmitters glutamate and D-serine are released to pre and post synapses in response to synaptic activity.

Their results show that it is possible to have astrocytic activation that leads to frequency dependent increase or decrease to synapse. Their mechanism is based on D-serine enhancing the effectivity of the postsynaptic NMDAR and glutamate depressing presynapse output. Their results also indicate that this kind of a mechanism could be responsible for bistable dynamics where the neuron shifts between two different frequency firing states. Their model indicates that the tripartite synapse functions as a kind of a high pass filter.

Astrocytes generating neuronal synchrony by Amiri et al.

The model by Amiri et al. (Amiri et al., 2012) consists of coupled Morris-Lecar models of neurons together with a dynamic model of an astrocyte. In the model, an increase of calcium concentration causes the release of astrocyte mediator. The astrocytes release ATP to inhibit the synaptic output of excitatory neurons mediated by adenosine which accumulates after the hydrolysis of released ATP. On the other hand, glutamate released by the astrocyte facilitates neurotransmitter release. They assume that when astrocyte calcium reaches a threshold an amount of gliotransmitter is released into the nearby synapse. Their model consists of single astrocytes controlling single synapses. In addition, the astrocytes are coupled with calcium flux to represent the gap junctions joining their cytosols.

Their simulations consisted of minimalistic network of 50 excitatory neurons and 50 inhibitory neurons. Astrocytes are placed in between the coupled excitatory and inhibitory neurons. The arrangement of the simulation can be seen in Figure 6.

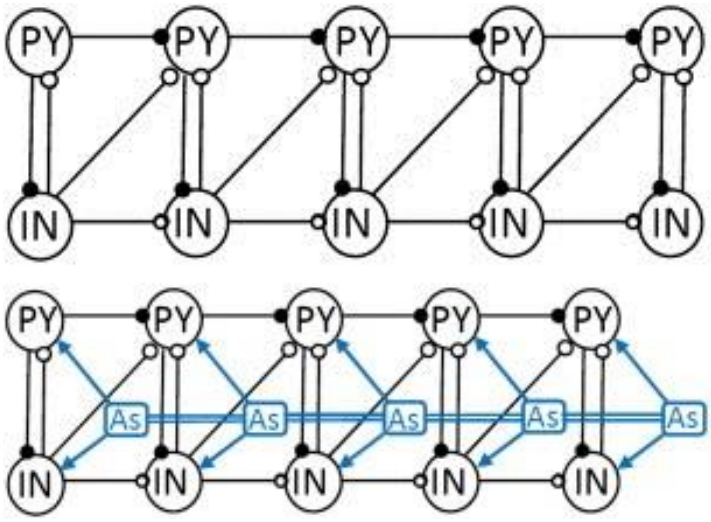

Figure 6: Simulation scheme by Amiri et al. White circles represent inhibitory synapses and black spheres represent excitatory synapses. Figure from (Amiri et al., 2012)***.***

Their results show that astrocytes in the network are able to shift the network between synchronous and asynchronous states.

Astrocytes as part of ANN classification by Porto-Pazos et al.

The last computational scheme described is not a model in the sense as the previously mentioned models. Artificial neuronal networks have been used in computer science for machine learning and classification problems before. However, those networks have only contained artificial neurons. Porto-Pazos et al. presented an artificial astrocyte-neuron network, where each neuron is connected to an astrocyte (Porto-Pazos et al., 2011). The astrocytes gradually increased the strength of the connection if there had been spikes and decreased it if there had not been. Spatial spread of the signal by gap junctions and calcium had not been taken into account.

Their results show that addition of slower time course dynamics of astrocytes into ANN increased the performance of the network in most classification tasks. After that they tested if the increase in performance was due to added elements in the system and increased the number of neurons in the neuronal network. However, similar increase in performance was not achieved.

2.3 Path to INEXA model

As discussed in the previous chapters, in the field of neuroscience the focus has been for long in neuronal networks and neuronal connections. In addition to neurons, the brain consists also of a large number of different other cell types. One of the main cell types are astrocytes representing roughly 50% of the cerebral volume (Kettenmann & Verkhratsky, 2008). The astrocytes form a part of blood-brain-barrier, interact with blood vessels and offer metabolic support to neurons. Until recently, the astrocytes connection to neurons were considered to be mainly metabolic support by regulating extracellular potassium (Volman, Bazhenov, & Sejnowski, 2012) and uptaking and degrading of neurotransmitters (Swanson & Graham, 1994). However, astrocytes have also been noted due to their ability to communicate with neurons directly and modulate neuronal communication. Part of the communication between a neuron and an astrocyte happens at the neuronal synapses, where the astrocyte wraps around the synapse forming so called tripartite synapse. The astrocytes have been found to perform complex functions and communicating with neurons through tripartite synapses using gliotransmitters. Release of gliotransmitters has been linked to astrocytes internal calcium pathways, and astrocyte dysfunction has been linked to many diseases like epilepsy and Huntington's disease (Maragakis & Rothstein, 2006; Seifert, Carmignoto, & Steinhäuser, 2010; Seifert & Steinhäuser, 2013; Volman et al., 2012).

Essentially gliotransmission consists of secretion of neurotransmitter molecules such as glutamate, GABA and ATP. Astrocytes release gliotransmitters like glutamate in response to synaptic activity. The astrocytes are also connected to each other by gap junctions. The gap junction forming proteins called connexins build a pore through the cell membranes of both cells joining their cytosols and letting through certain sized molecules (Fellin, 2009). Each of these systems is interconnected and as such has an effect to the

others. Each of these parts have been researched and also computational models of these subsystems have been developed (De Pittà et al., 2011; Lallouette et al., 2014; Lenk, 2011). However, there is no clear understanding about their joined function. In this work, we aim to develop a mathematical conceptual model of the combined astrocyte-neuron network modulation including all above parts of the astrocyte-neuron communication modeled in a biologically plausible way. In the model, we introduce for the first time a scheme, where each astrocyte is connected even up to hundreds of synapses and where astrocytes form a functional, calcium based communication network in parallel to the neuronal network.

3 METHODS

In this study, we take the best of the models found suitable for describing effects at different levels and combined them in a biologically reasonable way. Our hypothesis is that the astrocytes should promote bursting behavior in the neuronal network, while restrict hyperactivity. This would increase the operable range of neuronal activities where the network does not exhibit epileptic behavior but can still transmit signals. If the system can work in such a way, it could explain why a dysfunction in astrocytes can cause a certain disease. Our model aims to broaden the astrocyte's effect into large cells controlling multiple synapses and gathering their inputs.

3.1 Neuron-astrocyte network model INEXA

In this thesis, a model that integrates the above explained various parts of the astrocyte-neuron modulation was developed. The basis of the model was the neuronal network simulator INEX (Lenk, 2011). The simulator consisted of inhibitory and excitatory neurons and their connections based on inhomogeneous Poisson processes.

Here the model was further developed and a spatial topology was constructed using probabilistic functions. Cells were randomly placed on a virtual culture area and connected according to their distance from each other In order to model tripartite synapses, we used a modified version of the presynapse astrocyte interface by De Pittá et al. (De Pittà et al., 2011) for excitatory synapses. De Pittá's model is based on Tsodyks-Markram model synapse (Tsodyks & Markram, 1997), which we applied to all synapses. We made further modification to the presynaptic model that enables astrocytes to increase or decrease synaptic strength based on gliotransmission introduced by De Pittá et al. This modification takes into account different time scales of different transmitters and thus the effect gliotransmission depends on time scales. Astrocyte's IP_3 and calcium were modeled using simple exponential equations. Astrocyte calcium signaling between astrocytes was modeled by a simplified calcium signaling UAR model by Lallouette et al. (Lallouette et al., 2014). In order to combine the synaptic inputs from all the synapses belonging to a single astrocyte, each synapse area astrocyte's IP3 and calcium was summed up into one astrocyte's calcium response (Figure 7) and the total calcium of each astrocyte was modelled by Lallouette UAR model. In addition, each astrocyte was affected by IP_3 flow through gap junctions from connected astrocytes. The astrocyte's calcium leads to a signal back to the connected synapse. The astrocytes also released GABA to signal directly to INEX. Thus, the model integrated for the first time the neuronal network with presynaptic astrocyte effect and astrocyte calcium network into one system with a two-dimensional topology.

To demonstrate the model function and the role of the astrocytes in neuronal network level, we constructed the modeled one step at a time to see what affects each added stage had to the neuronal network behavior.

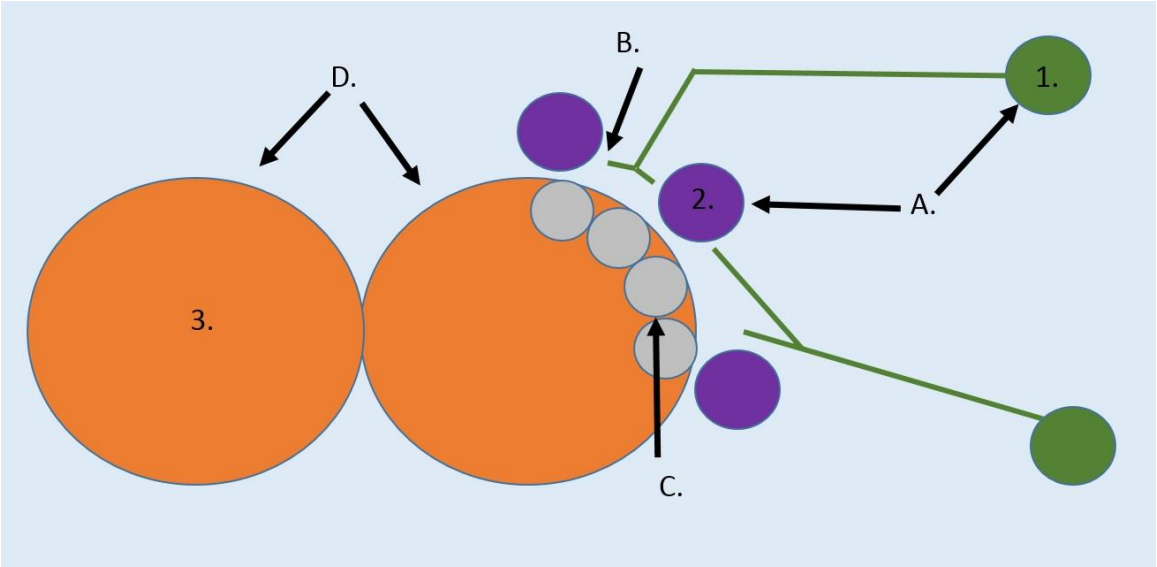

Figure 7: Schematic of the model. 1. Excitatory presynaptic neuron. 2. Postsynaptic neuron. 3. Astrocyte. A. INEX with neurons and connections. B. A version of Tsodyks-Markram model joined to each synapse with modified De Pittá astrocyte interface. C. Near synapse astrocyte simulators joined to each excitatory synapse the astrocyte it belongs to. D. Lallouette UAR simulator takes input from near synapse simulators and from other astrocytes.

3.2 INEX modifications

INEX was implemented as described earlier. In addition to the equations 3 and 4, the presynapse simulators were applied between each synapse connection as described in the next section. Also an additional inhibitory pathway was added from astrocytes to postsynaptic neurons through each excitatory synapse controlled by the astrocyte. This represents the astrocyte releasing GABA (y_{GABA}) to all nearby neurons. Equation 3 gets the following form for excitatory neurons:

$$11)\lambda_i(t_k) = \begin{cases} c_i + \sum_j y_{ij} \cdot s_j(t_{k-1}) + \sum_j y_{GABA} \cdot A_{ij}(t_{k-1}), & if\ c_i + \sum_j y_{ij} \cdot s_j(t_{k-1}) + \sum_j y_{GABA} \cdot A_{ij}(t_{k-1}) > 0 \\ 0, & otherwise \end{cases}$$

In the equation, A_{ij} denotes to if an astrocyte is in an active state that is connected to a synapse ij connected to the neuron. This indicates that the astrocyte is near enough that the GABA released by the astrocyte has an inhibitory effect to the postsynaptic neuron. The more connections there are, the closer and more encased in the astrocyte the neuron is and the stronger the effect.

In addition, the spike time history variable f was removed. To counteract the loss of activity in the network, the effect was applied all the time regardless if there was a spike or not and the basic activity of the network was reduced.

3.3 Presynapse

To implement the tripartite synapse into the INEX model, the synapses needed to be modeled in more detail. Since INEX uses a black box approach, it is possible to take part of the model out of the box and model it in more detail. Thus, we introduced the Tsodyks-Markram presynapse model (Tsodyks & Markram, 1997) in similar fashion as De Pittá et al. (De Pittà et al., 2011) have used it. The combination of the models was based on the idea that the synaptic strength of INEX is the total sum of effects starting from a spike and ending to axon hillock of the next neuron.

The Tsodyks-Markram model with the modifications by De Pittá et al. (De Pittà et al., 2011) was implemented as follows. In an event of a spike, $s_j(t_k)=1$, an amount of $U_{ij}(t_k)$ calcium enters the presynaptic terminal and binds to calcium receptors $\bar{u}_{ij}(t_k)$. An amount of $\bar{q}_{ij}(t_k)$ times $\bar{u}_{ij}(t_k)$ resources were released ($RR_{ij}(t_k)$), where $\bar{q}_{ij}(t_k)$ was the proportion of neurotransmitter vesicles ready to be released and $\bar{u}_{ij}(t_k)$ the calcium bound to the sensors (equation 12). Since calcium entering the terminal $\bar{u}_{ij}(t_k)$ depends on the amount of calcium present $u_{ij}(t_{k-1})$ and base amount of calcium $U_{ij}(t_k)$ entering the terminal, it will have smaller influx if there was calcium left from previous time slice $u_{ij}(t_{k-1})$ (equation 13). The amount of transmitters $\bar{q}_{ij}$ to be released at time t_k is the amount of transmitters q_{ij} at the terminal at the end of the previous time slice t_{k-1} (equation 14).

12) $\boldsymbol{RR_{ij}(t_k) = \bar{q}_{ij}(t_k) \cdot \bar{u}_{ij}(t_k) \cdot s_j(t_k)}$

13) $\boldsymbol{\bar{u}_{ij}(t_k) = \left(1 - u_{ij}(t_{k-1})\right) \cdot U_{ij}(t_k) \cdot s_j(t_k) + u_{ij}(t_{k-1})}$

14) $\boldsymbol{\bar{q}_{ij}(t_k) = q_{ij}(t_{k-1})}$

The amount of neurotransmitters Q_{ij} left at the synapse after spike was calculated from the amount of resources at the start of the time slice and resources released. If there was no spike, $RR_{ij}(t_k)$ was zero (equation 15). In both cases, a spike or no spike, a percentage of the used transmitters was replenished by $regenR$ percentage of missing resources over time Δt (equation 16) and percentage of $regenCa$ calcium is left at the terminal after each millisecond (equation 17). The regeneration was done as many times as there were milliseconds between the time slices and thus taken to the power of Δt.

15) $\boldsymbol{Q_{ij}(t_k) = \bar{\varrho}_{ij}(t_k) - RR_{ij}(t_k)}$

16) $\boldsymbol{q_{ij}(t_k) = Q_{ij} + (1 - Q_{ij}) \cdot regenR}$

17) $\boldsymbol{u_{ij}(t_k) = \bar{u}_{ij}(t_k) \cdot regenCa^{\Delta t}}$

Since the dynamics of the INEX model are based on constant synaptic strengths and the Tsodyks-Markram model has them variable, the only way to combine them was to consider steady state of the latter. I defined steady state as a state where the history of the synapse had no effect to the synaptic output. In steady state, where both the resources and calcium have time to settle near original value, the resources released are always the same. In this state, the synaptic output is independent of the history of the synapse and as such is in its base form. The formulas for this state are reduced from equations 12-14 to equations 18-20 and resulting in equation 21. Equation 18 is the same as equation 12, but since resources at the beginning of the time slice $q_{ij}(t_{k-1}) = 1$ and calcium left in the presynapse $u_{ij}(t_{k-1}) = 0$, the equations 13 and 14 are reduced to forms 19 and 20. The purpose of this was to show that the governing variable for neurotransmitter release amount was $U_{ij}(t_k)$ and then use this to combine the models.

18) $\boldsymbol{RR_{ij}(t_k) = \bar{\varrho}_{ij}(t_k) \cdot \bar{u}_{ij}(t_k) \cdot s_j(t_k)}$

19) $\boldsymbol{\bar{u}_{ij}(t_k) = U_{ij}(t_k)}$

20) $\boldsymbol{\bar{\varrho}_{ij}(t_k) = 1}$

21) $\boldsymbol{\rightarrow RR_{ij}(t_k) = U_{ij}(t_k) \cdot s_{ij}(t_k)}$

From equation 21 could be seen that $U_{ij}(t_k)$ is the governing variable for steady state and that in the event of a spike, amount of $U_{ij}(t_k)$ calcium entering the synapse determines alone the amount of resources to be released. To our convenience, the value for $U_{ij}(t_k)$ was a real number between 0 and 1, just as the synaptic weights for INEX have when using a maximum upper boundary of 1. Since the upper boundary can be set to any value from 0 to 1, the highest release amount was set to the highest boundary value set in INEX, UB_{max} using equations 22 and 23. The purpose of this was to be able to scale the strength of the synapse based on synaptic strengths at INEX and independently of a set synaptic strength for full release.

To combine INEX and the synapse simulation, a base value of the synapse given at INEX, $y_{ij_{base}}$was determined as the original synaptic strength set to a synapse in the initialization of INEX. The strength remains between 0 and its respective upper boundary value. Both y^{+}_{ji} and y^{-}_{ji} boundaries will be lower or equal to the higher one of the two boundaries called UB_{max}. Also the value $y_{ij_{base}}$ will be lower or equal to UB_{max}, since the synaptic strengths are selected with triangular distribution between 0 and the respective boundary. Both boundaries are lower or equal to the higher of the boundaries.

This means that the highest possible effect from releasing all the transmitters in the synapse should result in synaptic strength of UB_{max}. The input from the INEX is scaled between 0 and 1 by dividing the base value of the synapse by the maximum release boundary as shown in equation 23. In the steady state special case, according to equations 19 and 20 and based on equation 21 the output $RR_{ij}(t_k)$ is exactly $U_{ij}(t_k)$. To scale the value back between the INEX boundaries, the resources released was multiplied with UB_{max} (equation 22). In steady state, the UB_{max} canceled itself out and the final result was $y_{ij_{base}}$ as it should be. However, when the synapse is not in steady state it can gain resources released values that result in $y_{ij}(t_k)$ values that are higher or lower than $y_{ij_{base}}$, but between 0 and UB_{max}.

$$\textbf{22)}\ y_{ij}(t_k) = \begin{cases} s_j(t_k) = 1 : RR_{ij}(t_{k-1}) \cdot UB_{max} \\ s_j(t_k) = 0 : y_{ij_{base}} \end{cases}$$

$$\textbf{23)}\ U_{ij}(t_k) = \frac{y_{ij_{base}}}{UB_{max}}$$

An example of scaling the output has been shown graphically in Figure 8.

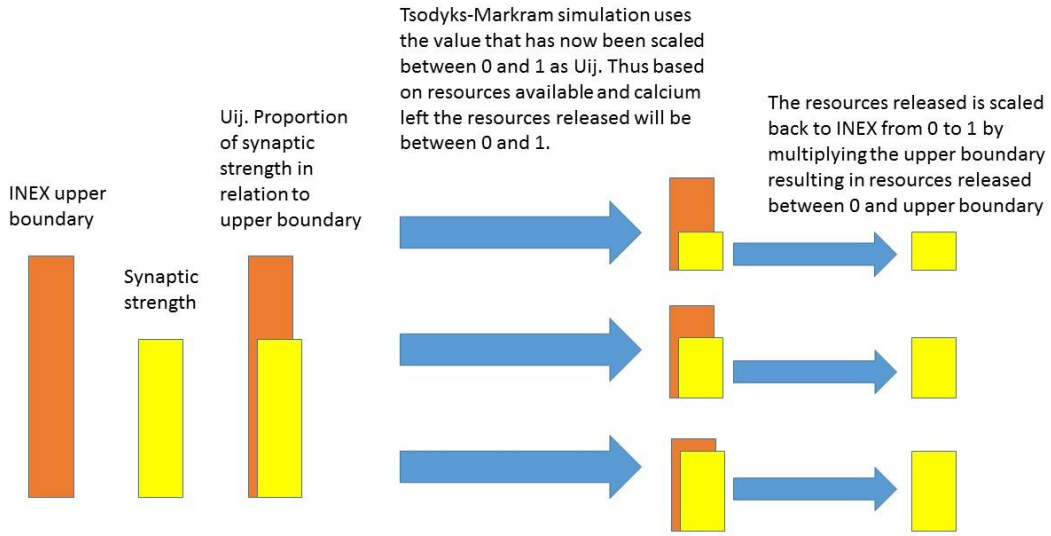

Figure 8: Visualization of the combination of the models. The upper boundary UB_{max} is the absolute maximum a synapse can have as its strength. Thus the synaptic strength in relation to UBmax is a value between 0 and 1. This value is then used as Uij of the Tsodyks-Markram simulation to make it independent of the actual synaptic strength values used by INEX. The output of the synapse is between 0 and 1 and this is scaled back to INEX by multiplying the value by UB_{max}.

With tripartite synapses, the transmitter release is also detected by the astrocyte (De Pittà et al., 2012; Fellin, 2009; McIver et al., 2013; Min, Santello, & Nevian, 2012). For glutamatergic synapses, the astrocyte uses mGluR to detect the signaling. The mGluR

cleaves IP_3 from Phosphatidylinositol 4,5-bisphosphate (PIP_2) (Figure 9). This signaling molecule is detected by receptors at the endoplasmic reticulum (ER). IP_3 causes a release of calcium from the cells internal calcium stores in the ER (De Pittà et al., 2012, 2011; Hirase, Iwai, Takata, Shinohara, & Mishima, 2014; Lalo et al., 2014; Min et al., 2012; Sahlender, Savtchouk, & Volterra, 2014; Veletić, Mesiti, Floor, & Balasingham, 2015; Volman et al., 2012) which causes in turn more calcium release through calcium induced calcium release (De Pittà et al., 2012; Veletić et al., 2015). This is suggested to be related to gliotransmitter release.

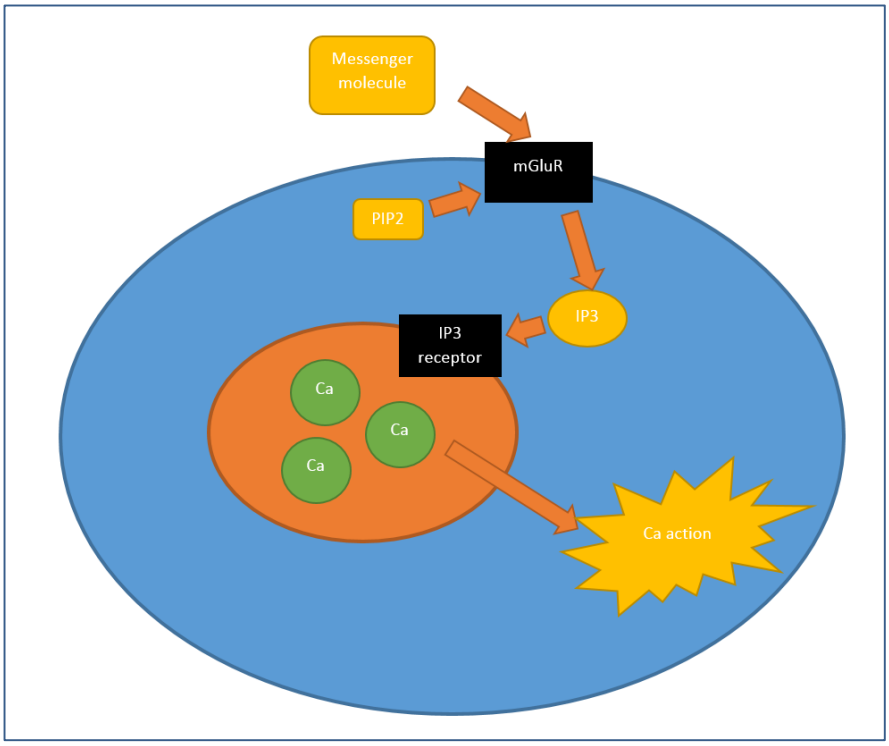

Figure 9: Astrocytes internal IP3 mediated calcium pathway.

It has been seen that the calcium signaling in astrocytes can be of two main types. First of all, the full cell calcium signal can happen on its own, independent of neuronal activity. The other type is activity driven calcium signaling (Perea, Navarrete, & Araque, 2009; Wallach et al., 2014). In some cases, the activity driven calcium signaling does not reach the whole cell level but is contained near the synapse and causing calcium rise only locally at only one or few synapses range (Perea et al., 2009).

To form our hypothesis of how the different transmitters are released, we need to look into what each of these transmitters is known to do. When CA3-CA1 hippocampal synapses were treated with fluorocitrate (FC) the astrocytic glutamate release is diminished. As a result paired pulse facilitation takes place together with reduced postsynaptic potency and reduced release probability. FC also decreases intracellular calcium signaling (Bonansco et al., 2011). This would suggest that glutamate increases the synaptic transmission as it has been shown that NMDARs can facilitate the synapse

(Jourdain et al., 2007; Larrosa et al., 2006). NMDARs are known for their possible role in long term potentiation and learning at the postsynaptic side (Min et al., 2012), but it turns out that there are also extrasynaptic NMDARs, which are located outside the synapse (Bonansco et al., 2011; De Pittà et al., 2012, 2011; Fellin, 2009; Papouin & Oliet, 2014). These receptors are thought to be the target for astrocytic glutamate and the mediator of small inward currents (Parri, Gould, & Crunelli, 2001).

In addition to NMDARs, the synaptic potency is increased by metabotropic glutamate receptors (Perea & Araque, 2007). Thus glutamate works through two different receptors to potentiate the synaptic transmission.

Astrocytes also release ATP, which acts as a gliotransmitter at the presynapse through purinergic receptors. ATP is also suggested to act as an extracellular messenger for transmitting calcium waves between astrocytes. Moreover, ATP is hydrolyzed into adenosine (Hines & Haydon, 2014), which acts on A1 receptors at the presynapse by reducing synaptic strength.

For modeling the tripartite synapse, we followed the paper by De Pittá et al., were a single parameter was used to describe the effects of co-operation of multiple receptors. This effect parameter is called the alpha parameter. We used an interface very similar to that described in the paper by De Pittá et al. (De Pittà et al., 2011) between near synapse areas and the presynapse. Thus, we counted the effect of different receptors as a lumped sum of their effects. To do this, we considered that the ATP and glutamate were released in a single release event and that their kinetics at the receptors were fairly similar. The receptors together determine the base level of synaptic modification under gliotransmission. However, all inhibitory and excitatory synapses still follow the Tsodyks-Markram dynamics.

Presynapse model modifications

Alpha parameter was implemented as described by De Pittá et al. The value of alpha is determined by the combination of presynaptic receptors.

The effect of the alpha parameter is shown in equation 24, where $U_{ij\alpha}(t_k)$ describes the new $U_{ij}(t_k)$ after taking into account the effects of gliotransmission and $g_{ij}(t_k)$ the amount of bound gliotransmitters at the presynaptic receptors.

$$\textbf{24)}\ \boldsymbol{U_{ij\alpha}(t_k) = \frac{y_{ij_{base}}}{UB_{max}} \cdot \left(1 - g_{ij}(t_k)\right) + \alpha \cdot g_{ij}(t_k)}$$

This means that $U_{ij\alpha}(t)$ which now governs the synaptic release instead of $U_{ij}(t_k)$ in equation 23, corresponds to the synaptic weight of $RR_{ij}(t_k) = U_{ij\alpha}(t_k) = \frac{y_{ij_{base}}}{UB_{max}}$ in steady state as in equation 21 as long as there is no gliotransmission. In the equation full release of 1 corresponds to the synaptic strength at the highest upper boundary as it should

be. In such a case $y_{ij_{base}} = UB_{max}$ and according to equation 24 without gliotransmission $U_{ij\alpha}(t_k) = 1$.

When gliotransmitters are introduced, the synapses strength shifts proportionally towards alpha times UB_{max}. With these mechanics, astrocyte gliotransmission can both increase and decrease synaptic output within the natural limits set by Tsodyks-Markram dynamics. The strength of the synapse changes depending on gliotransmission and previous activity.

Presynapse-astrocyte connections

Each astrocyte has been divided into local areas comprising area around a synapse and the rest of the cytosol forms the other part. In the model, every excitatory synapse has its own near synapse calcium dynamics. These dynamics are governed by two variables. First, at an event of synaptic transmission, the astrocyte responds with ionositoltrisphosphate $IP_{3_{ij}}(t_k)$ increase. This value is used together with the calcium variable to slow down the astrocytes response. The IP_3 is decreased over time by degrading factor $IP_{3_{dg}}$. New spikes at the presynapse will produce more $IP_3(t_k)$ signal. The increase at an event of a spike is dependent on previous $IP_3(t_{k-1})$ as well as amount of resources released into the synaptic cleft $RR_{ij}(t_k)$ as shown in equation 25.

The gliotransmission is governed by local astrocyte calcium concentration described as near synapse calcium $Ca(t_k)$. The previous level of $Ca(t_{k-1})$ is changed towards $IP_3(t_k)$ by the amount of the difference of the values times an accumulation factor acc. There is no calcium degrading term but instead it will follow the IP_3 variable with a small delay to increase or decrease Ca (equation 26). This is done because the calcium release machinery is expected to function in the scale of hundreds of milliseconds and the simulation is run in 5ms intervals.

When the near synapse calcium exceeds a set threshold, gliotransmission occurs. There are no more gliotransmission events at that synapse until the set threshold is met again after near synapse calcium has dropped below the threshold $\mathrm{Ca_{th}}$ (Equation 27). In this equation, the threshold is represented by Ca_{th}, the gliotransmitter amount by $g_{ij}(t_k)$, the gliotransmitter release proportion by g_r and the transmitter degrading term by g_{dg}. The transmitter is degraded over time.

$$\textbf{25)}\boldsymbol{IP_{3_{ij}}(t_k)} = \begin{cases} \boldsymbol{s_j(t_{k-1}) = 1 : IP_{3_{ij}}(t_{k-1}) \cdot IP_{3_{dg}} + \left(1 - IP_{3_{ij}}(t_{k-1}) \cdot IP_{3_{dg}}\right) \cdot RR_{ij}(t_k)} \\ \boldsymbol{s_j(t_{k-1}) = 0 \ : \ IP_{3_{ij}}(t_{k-1}) \cdot IP_{3_{dg}}} \end{cases}$$

$$\textbf{26)} \ \boldsymbol{Ca_{ij}(t_k) = Ca_{ij}(t_{k-1}) + (IP_{3_{ij}}(t_k) - Ca_{ij}(t_{k-1})) \cdot acc}$$

$$\textbf{27)} \ \boldsymbol{if \ Ca_{ij}(t_k) > Ca_{th}} \ \&\& \ \boldsymbol{Ca_{ij}(t_{k-1}) < Ca_{th}}$$

$$\rightarrow g_{ij}(t_k) = \left(g_{ij}(t_{k-1}) + \left(1 - g_{ij}(t_{k-1})\right) \cdot g_r\right) \cdot g_{dg}$$

$$else \quad g_{ij}(t_k) = g_{ij}(t_{k-1}) \cdot g_{dg}$$

Unlike in the model by De Pittá et al., this model uses a fixed gliotransmission release proportions for simplification.

3.4 Astrocyte-neuron network spatial topology

We assume that in the case of high activity it would be possible to get even higher activity through glutamate acting on mGluR and NMDAR. We assume that GABA is released during the full astrocyte signaling to counteract excess activity. Since this type of signaling is related to astrocyte location we needed a model with topology. To model the astrocyte calcium signaling, we used the UAR model introduced by Lallouette et al.(Lallouette et al., 2014). The UAR model consists of an interconnected network of astrocytes. In the network each astrocyte is a node and gap junctions form connections between the nodes.

To get a spatial distribution, the astrocytes were randomly placed on a virtual culture area. If two astrocytes are found to be closer to each other than a set minimum distance, one of them is randomly moved again until all the astrocytes are far enough from each other. Each astrocyte is connected by cap junctions to all neighbors within the maximum connection distance of 100µm. This represents the approximate diameter of one astrocyte. The spatial topology of neurons was built the same way as for astrocytes. However, the method for connecting the neurons differs. Since neurons are able to form long distance connections a probability of connection is set by a scaled Gaussian distribution shown Figure 10.

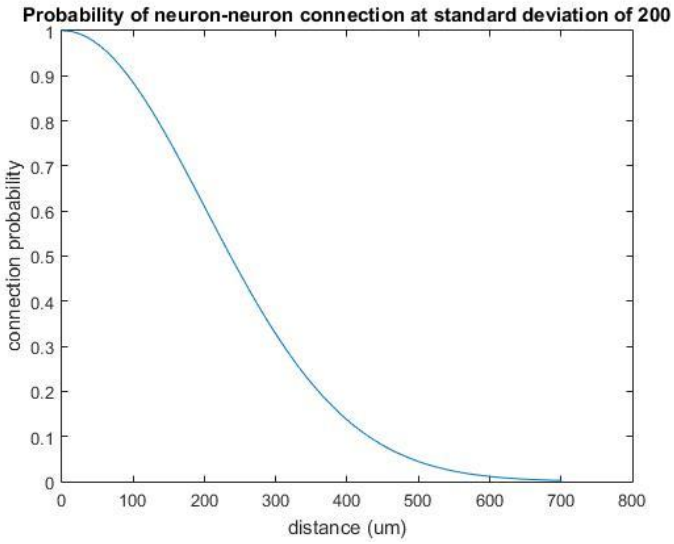

Figure 10: Probability of a neuron being connected to another neuron based on the distance between the two neurons. The connection will be determined separately for both directions.

The connection of astrocytes to neurons was defined using a combination of the two previous methods. The synapses are connected to the nearest astrocyte by a probability distribution similarly to that of used to connect neurons (Figure 11: Connection probability for each synapse to the nearest neuron. If the synapse is found not to be connected to the nearest, the second to nearest is tested until distance limiter of astrocyte size is reached. The astrocytes further than that are not able to connect to the synapse due to them not being able to contact the synapse. The difference is of course the extent to which the astrocytes can connect to the synapses thus the distribution is a scaled Gaussian with a hard set limiter at 70 µm to represent an absolute maximum distance after which there are no astrocyte processes to contact with. If the synapse is not connected to the nearest astrocyte, the next one is tried and so forth. This represents the astrocyte processes being entangled at the edges of the astrocytes. This also leaves it possible for an excitatory synapse to be left without an astrocyte and thus not forming a tripartite synapse. In this case, it functions only with the Tsodyks-Markram synapse without any astrocyte interface.

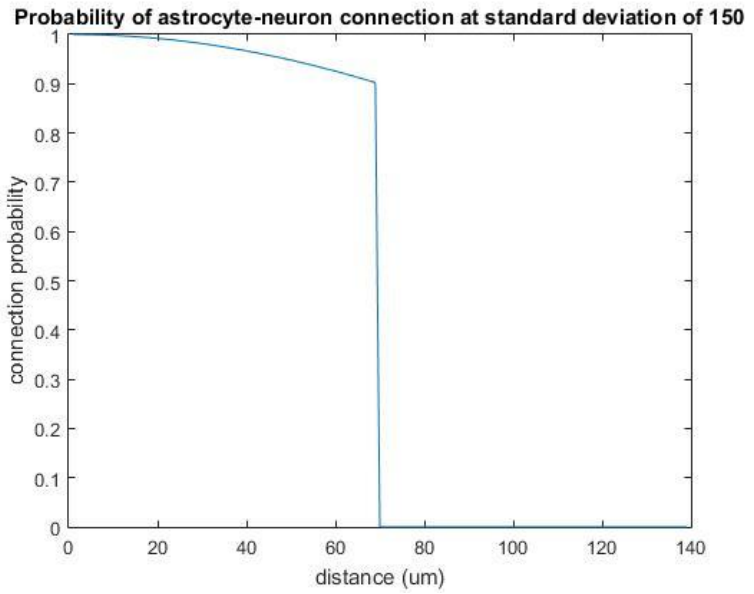

Figure 11: Connection probability for each synapse to the nearest neuron. If the synapse is found not to be connected to the nearest, the second to nearest is tested until distance limiter of astrocyte size is reached. The astrocytes further than that are not able to connect to the synapse due to them not being able to contact the synapse.

3.5 UAR model modification

As described earlier the UAR model is a cellular automaton describing calcium signaling states of astrocytes. In our model we use UAR as

$$28)\ flux_{a\ in}(t_k) = \sum flux_{b\ out}(t_k) + \frac{\sum Ca_j}{N} \cdot M$$

Equation 28 describes the IP_3 fluxes into an astrocyte that were summed up. The equation replaces equation 6 from the UAR model. The average of the time delayed variable at the

near synapse areas multiplied by a scaling variable M was added to the fluxes. This internal flux can cause the astrocyte to start calcium signaling based on neuronal activity it detects.

When the astrocyte is active it has high internal calcium and IP_3. This is signaled back to near synapse area simulators by setting IP_{3ij} to one for the duration of the active state. Also every excitatory synapse that was connected to the astrocyte form an inhibitory signal to the postsynaptic neuron in INEX. This represents astrocyte releasing GABA when the whole cell is active.

3.6 Simulations

To demonstrate the function of the model and the effect of each component to the network simulation the model components were added to INEX in three different stages. Each stage simulations consisted of INEX network with same basic properties simulated with three different basic activity in neuronal network. The network consists of 250 neurons of which 200 are excitatory and 50 inhibitory. This gives us 80% excitatory and 20% inhibitory neurons.

The simulator was run in different settings to get values for each added stage of the simulator. Each phase produced three sets of data that were analyzed. To test the effect of the number of astrocytes on the network activity we used in phase four simulated cultures with roughly 10%, 20% and 30% astrocytes, respectively. At each level of astrocytes the astrocyte network is formed anew but the same neuronal network was used in all simulations. Thus these four phases produced 18 simulation scenarios. Simulation time of 5 minutes was chosen and simulation run with 5ms time intervals. The simulations were analyzed using spike counts and discrete Fourier transforms (DFT).

The parameters used in the simulations can be found at the table in Appendix 1.The simulations were run on Merope-cluster using mainly partitions parallel and bigmem (Appendix 2). Merope used on default MatlabR2013b. The results were analyzed on home PC using Matlab R2015a.

4 RESULTS

The simulations were run in four phases. At the first phase the simulator was run with only noise and having synaptic strengths at zero to see the noise in the system. In the second phase INEX with Tsodyks-Markram presynapse simulators were added to see the response of the neuronal network to the noise. In the third phase presynapse area astrocytes were added to see their effect. In the final phase astrocyte networks were formed over the neuronal network. Twenty-eight, 63 and 107 astrocytes were added to each noise level simulation corresponding to 10%, 20% and 30% astrocyte proportions of all the cells. Graphs contain spike trains of all 250 neurons and below them graphs showing pooled spike counts are drawn with red. The results of the DFT are shown in separate figures. It is important to note that the frequencies of the DFT are not the frequencies of the neurons but the frequencies describing the behavior of the pooled spiking activity.

4.1 Phase 1: Noise

The networks in phase one are driven by basic activity of the neurons. The resulting noise in neurons is shown for low, medium and high basic activity in Figure 12. This was achieved by setting synapses to have no effect to the spiking of the next neuron. All 250 neurons have their spike trains plotted in black at the top of each graph. Below them are pooled spike counts for each time slot.

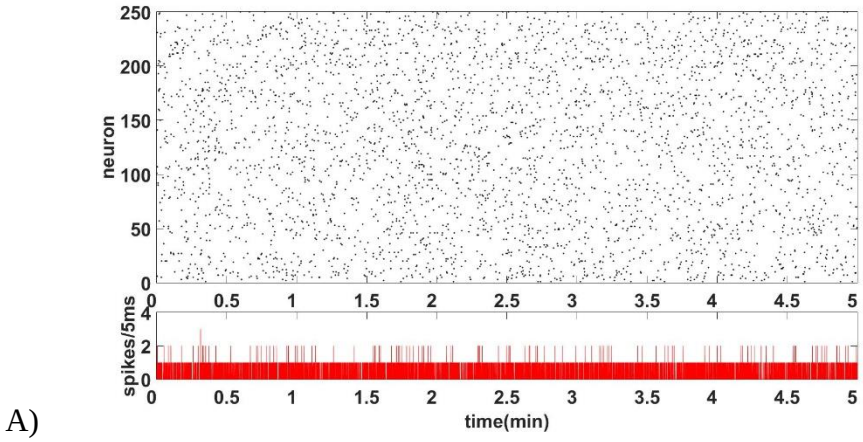

A)

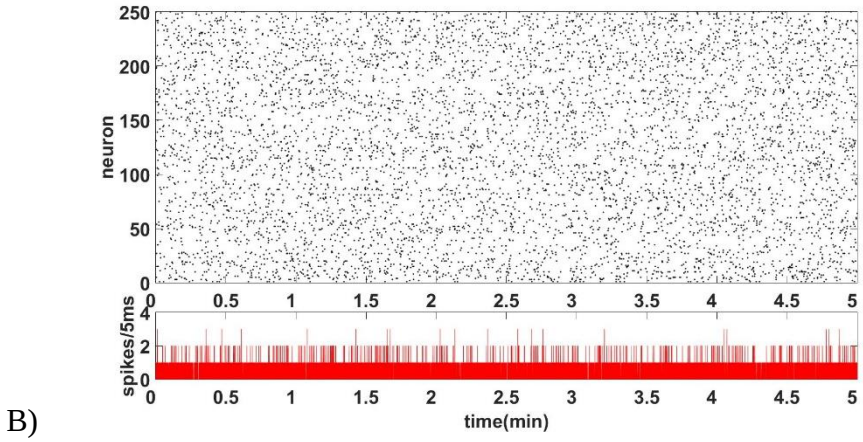

B)

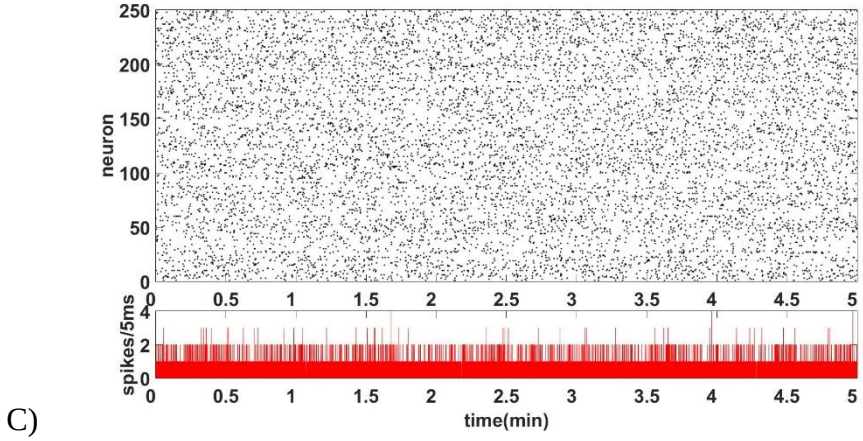

C)

Figure 12: Phase 1. Resulting noise from low (A), medium (B) and high (C) basic activity. Black graphs on top show spike trains of all 250 neurons for 5 minutes. The graphs below show pooled spike counts for each 5ms.

Running DFT for the noises show that the very low frequency component at the left side corresponds to noise amount (Figure 13). The power of the low frequency component is roughly 0.023 for low, 0.042 for medium and 0.063 for high noise. Other than that the relative power ratios look very much alike Figure 13: Phase 1. DFT graphs of the spike counts resulting from low (A), medium (B) and high (C) noise.

A)

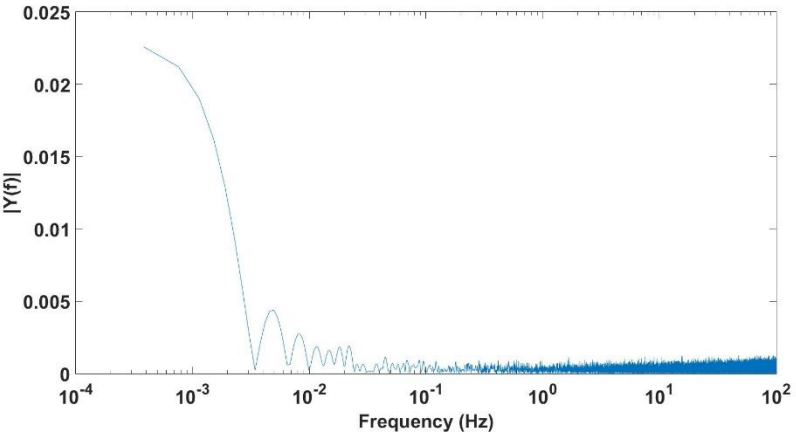

B)

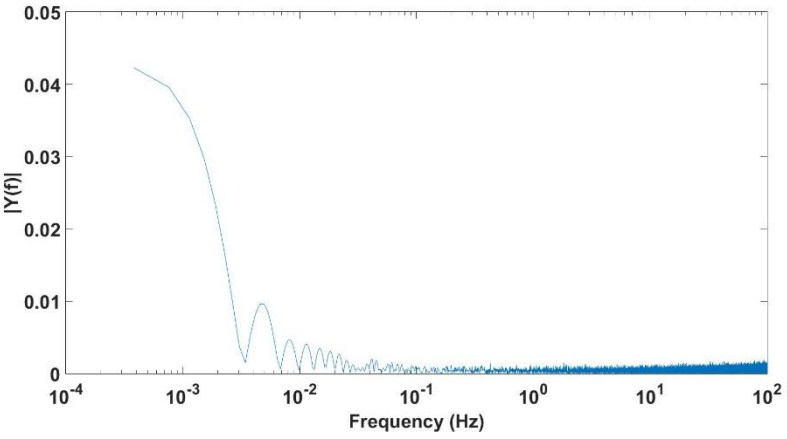

C)

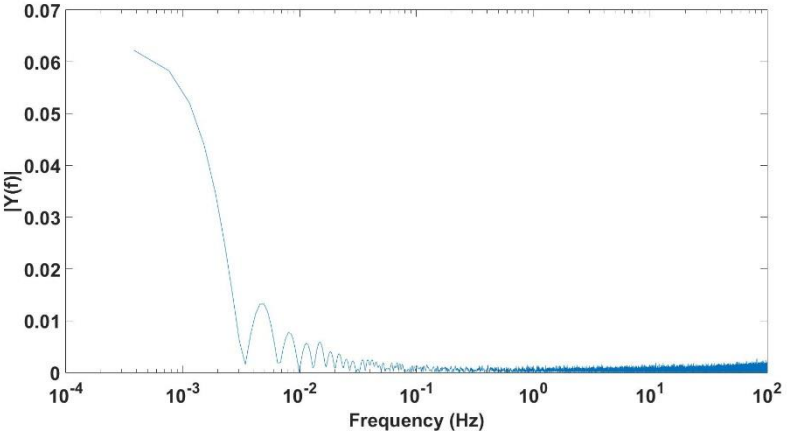

Figure 13: Phase 1. DFT graphs of the spike counts resulting from low (A), medium (B) and high (C) noise. The blue graph shows the power of each frequency component needed to reproduce the spike count graph.

4.2 Phase 2: Neuronal network

At phase two INEX with Tsodyks-Markram simulator was added to see the response of the neuronal network to the noise. Figure 14 shows the responses of the neuronal network. However while it is possible to see population burst like activity in the low (A) and even

some on medium (B) noise levels, the high activity result (C) looks mainly amplified noise.

A)

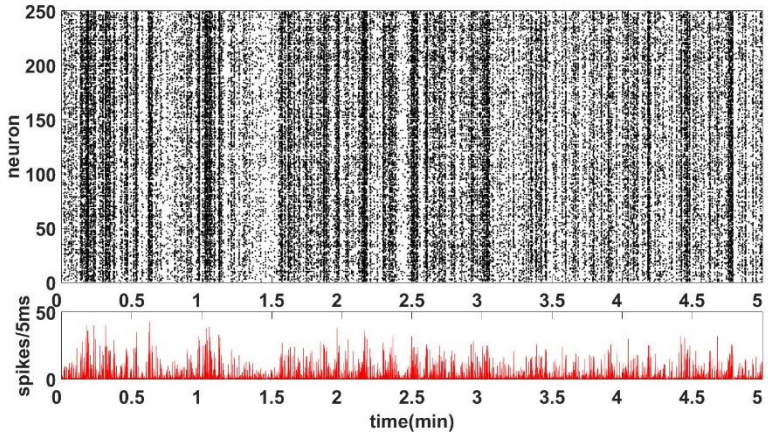

B)

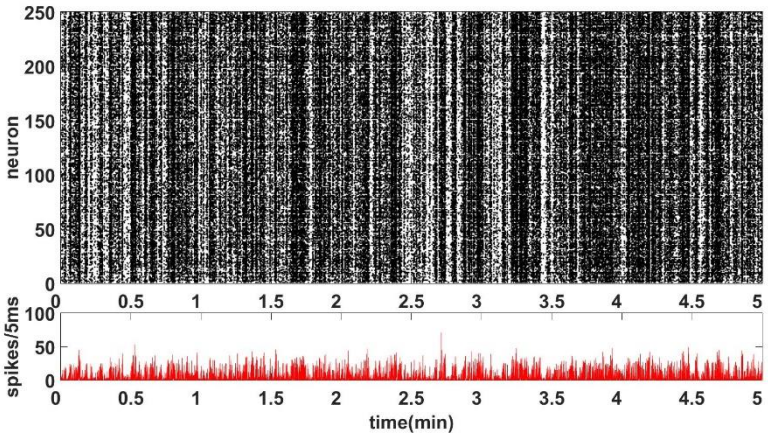

C)

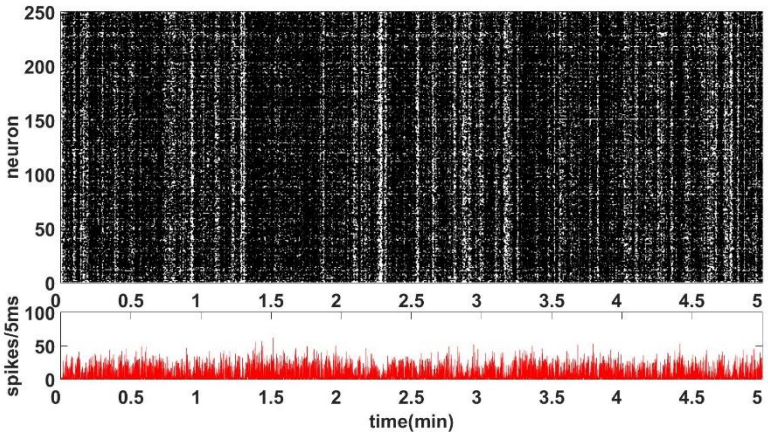

Figure 14: Phase 2. Neuronal network response to low (A), medium (B) and high (C) noise.

The DFT results in Figure 15 show the same development as the noise with the very low frequency component as for noise. In the DFT results the low and partly medium noise

response can be seen as higher relative power components in the 10^{-2} to 10^{-1} and even higher frequencies indicating more complex signaling behavior.

A)

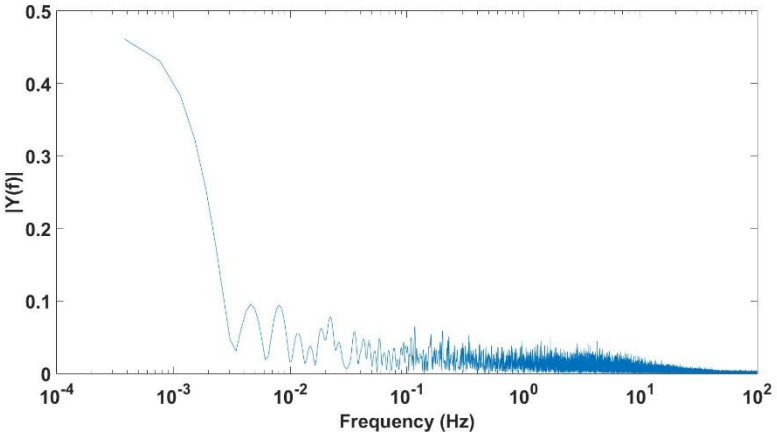

B)

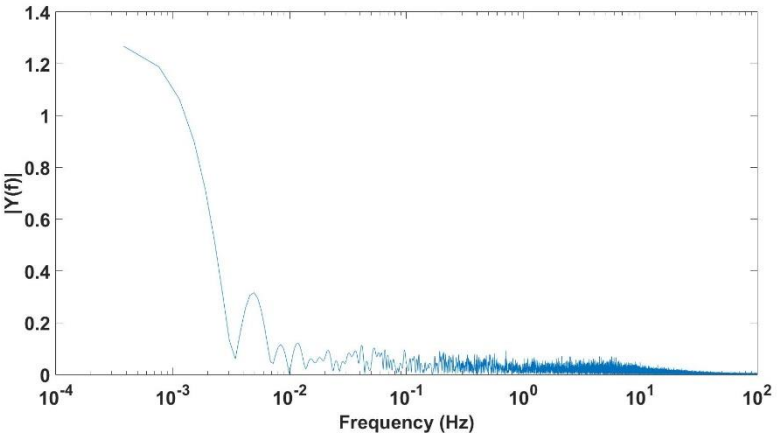

C)

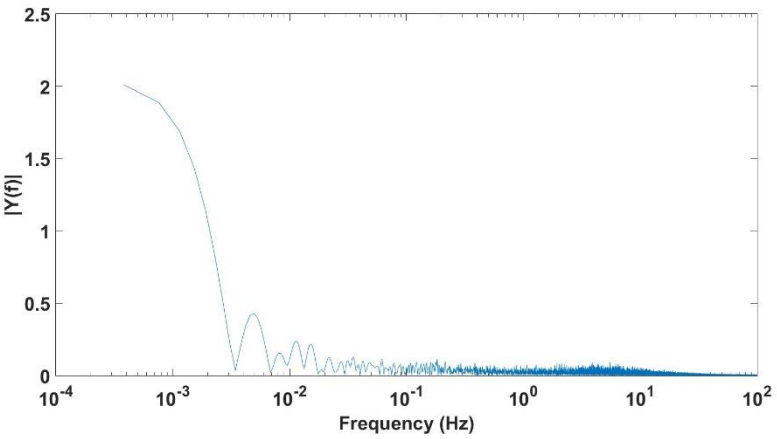

Figure 15: Phase 2. DFT of neuronal network spikes with low (A), medium (B) and high (C) noise.

4.3 Phase 3: Presynapse area astrocyte simulation

Addition of presynapse area astrocytes in phase three with alpha value higher than average synapse strength shifts all the noise levels to higher activity (Figure 16). They all resemble more the neuronal network response to high noise (Figure 14 C) than their corresponding neuronal network results (Figure 14).

A)

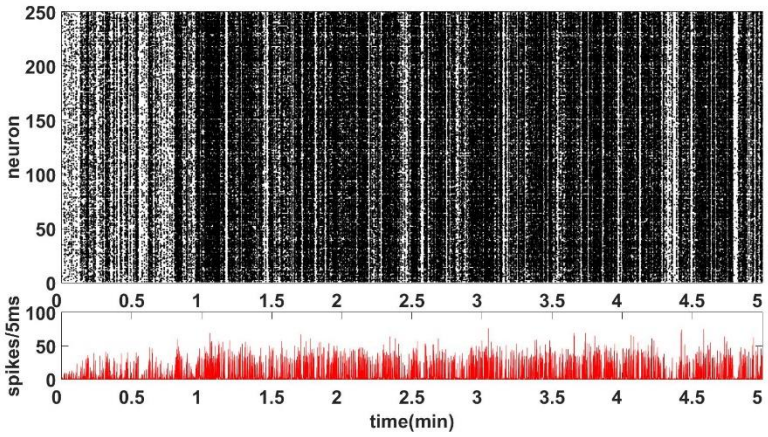

B)

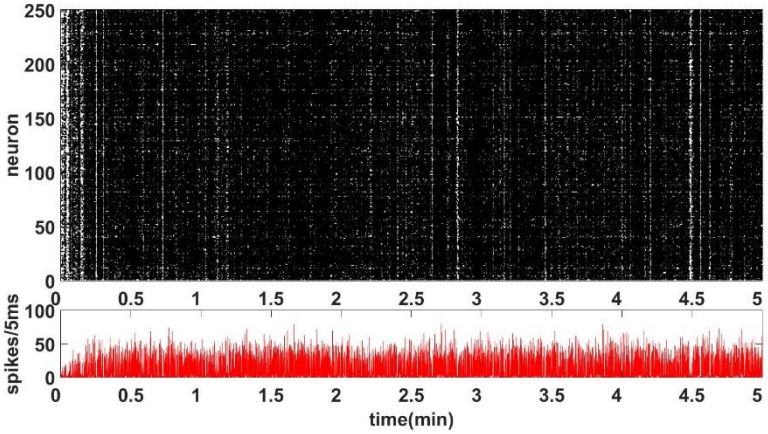

C)

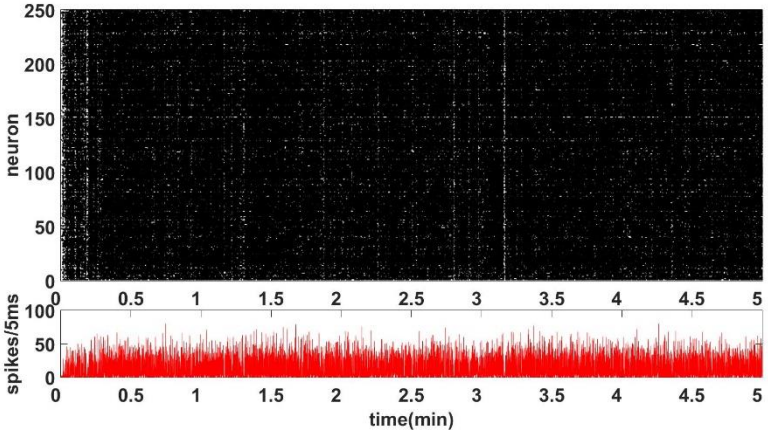

Figure 16: Phase 3. Presynapse area astrocytes added. Low (A), medium (B) and high (C) noise responses.

From the DFT graphs of the phase 3 the same phenomena can be seen as before. When population burst like behavior can be seen in the spike trains it is also visible in the 10^{-2} to 10^{-1} region of the DFT (Figure 17). The DFT results of medium and high noise responses are very similar to those of noise (Figure 13) but with higher total power.

A)

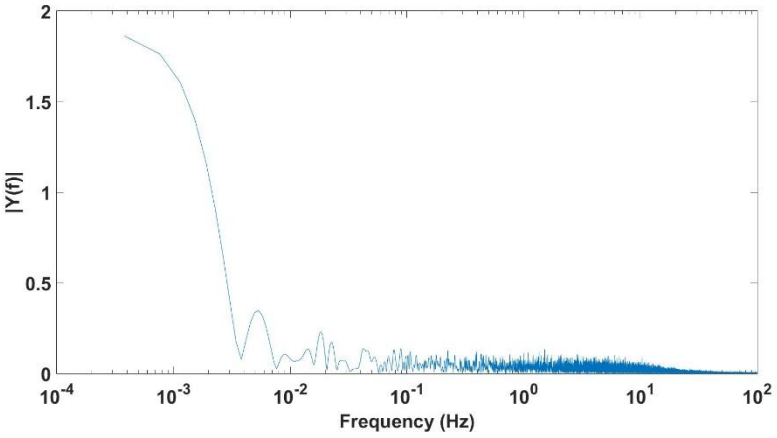

B)

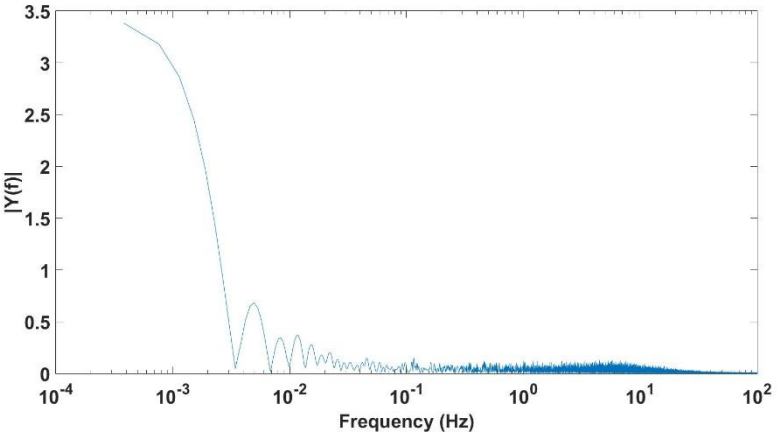

C)

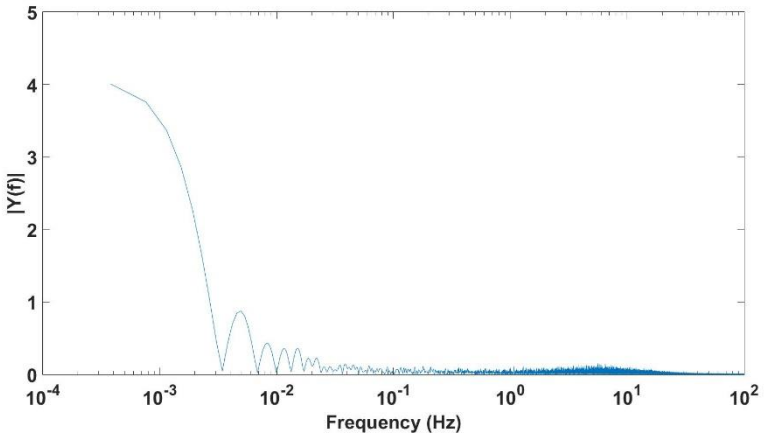

Figure 17: Phase 3. DFT of neuronal network spikes with presynapse astrocytes with low (A), medium (B) and high (C) noise.

4.4 Phase 4: INEXA

In phase four, the full INEXA model was implemented with different amounts of astrocytes. The results in this section are divided into three subsections each containing three simulation runs with different noise levels. Each simulation was analyzed separately as before. In addition the network topology was drawn and the amount of active astrocytes traced. The topology is represented with wire frame, where dots present the approximate location of the cell soma and wires the gap junction connections between the cells. Active astrocytes were pooled the same way as spike counts.

4.4.1 10% Astrocytes

First 28 astrocytes were added to get a mixture of cells having 10% astrocytes. Two-hundred excitatory neurons, 50 inhibitory neurons and 28 astrocytes totals up 278 cells of which 28 astrocytes corresponds to roughly 10%. Figure 18 shows the formed astrocyte network. As it can be seen from the figure this amount of astrocytes do not really form a connected network.

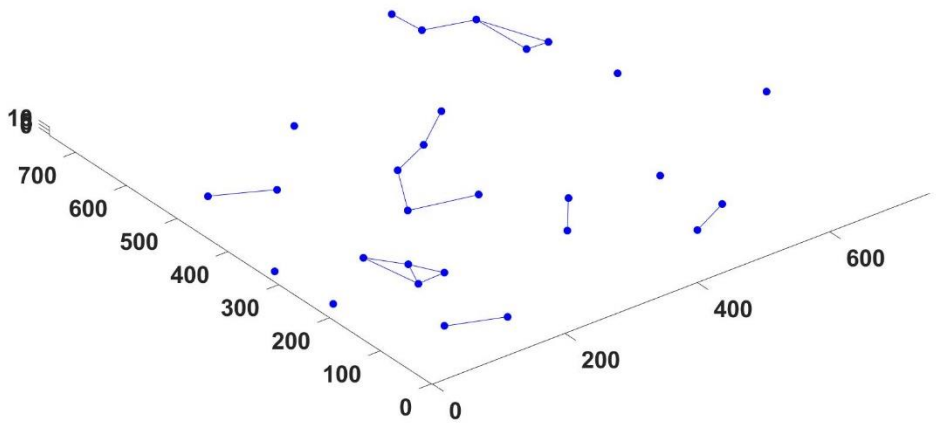

Figure 18: Astrocyte network formed by 28 astrocytes. Culture space is 750µm a side and 10 µm deep.

The response after adding the full INEXA model with 10% astrocytes for low noise (Figure 19 A) seems to bring the response closer to that of the neuronal network without astrocytes. This can be seen clearly from Figure 20 where the three different stage spike trains and DFT results are presented side by side.

A)

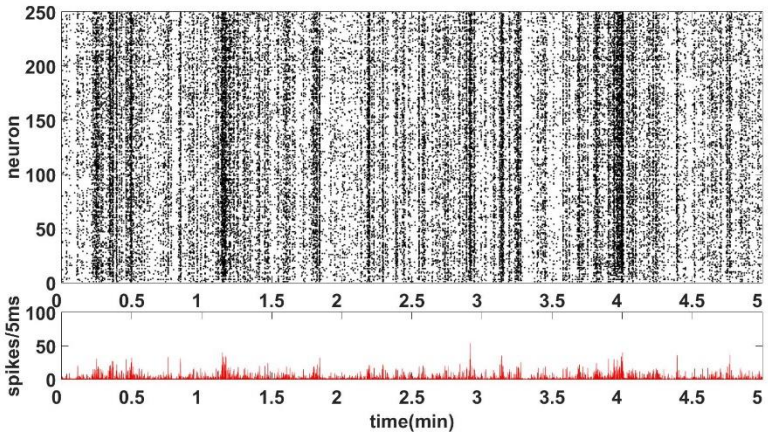

B)

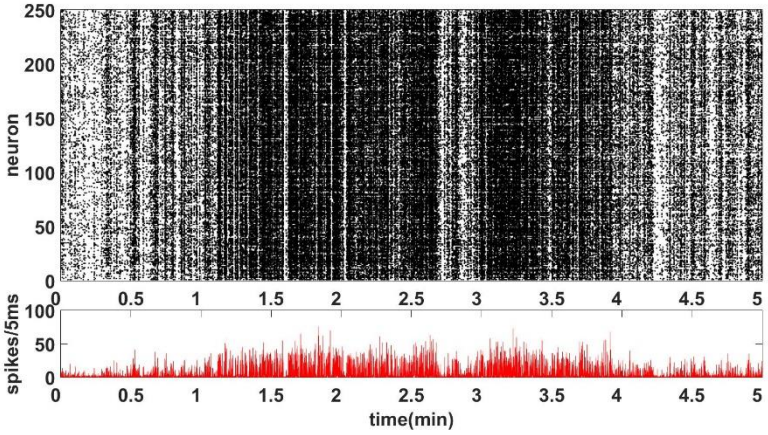

C)

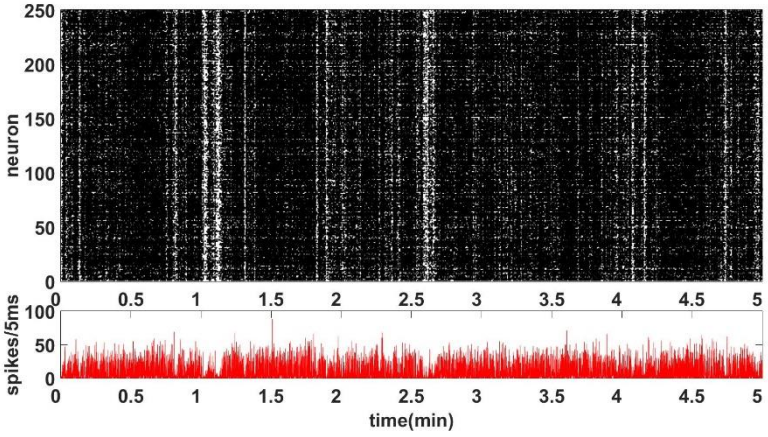

Figure 19: Phase 4. INEXA with 10% astrocytes. Low (A), medium (B) and high (C) noise responses.

A)

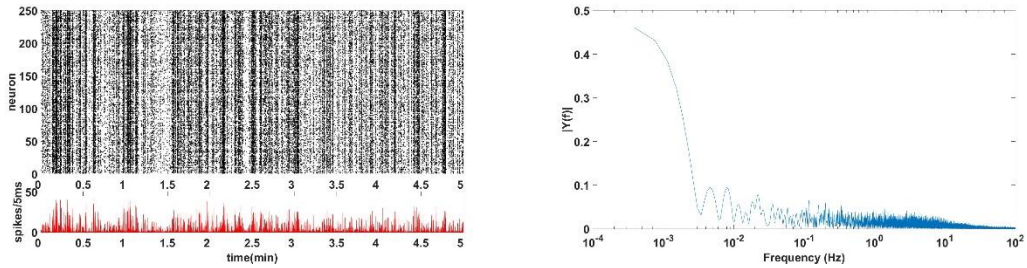

B)

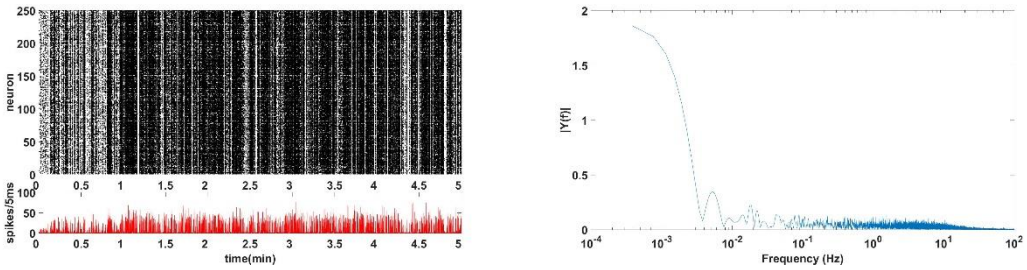

C)

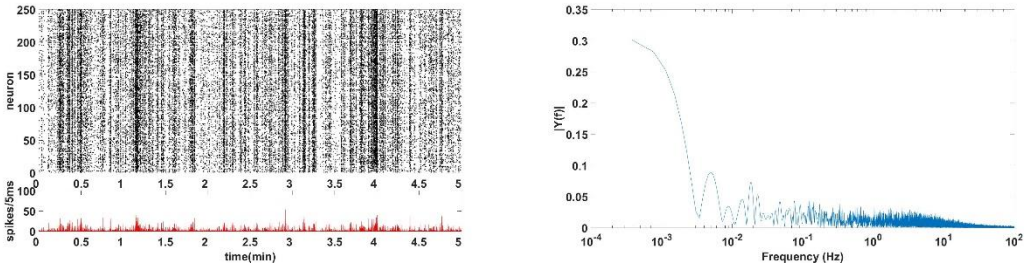

Figure 20: Comparison: Spike trains and DFT of phase 2 (A), phase 3 (B) and phase 4 with 10% astocytes (C) in response to low noise. There were higher absolute spike counts in the bursts with astrocytes (C) resulting in spike pools axis being higher than with neuronal network only (A).

The DFT results of the responses to medium and high (Figure 21 B and C) look more similar to those of their corresponding noises (Figure 13 B and C) and the results from phase 3 simulations (Figure 17 B and C) than the population burst containing low noise results (Figure 21 A). As can be seen from the DFT in Figure 21 A it has higher relative power in the 10^{-2} to 10^{-1} region than the noise (Figure 13 A) just as with the pure neuronal network (Figure 15 A). Similarly in medium and high noise simulations (Figure 19 B and C) the astrocytes try to restrict the hyperactive network by GABA releases, but they are not strong enough to prevent it.

A)

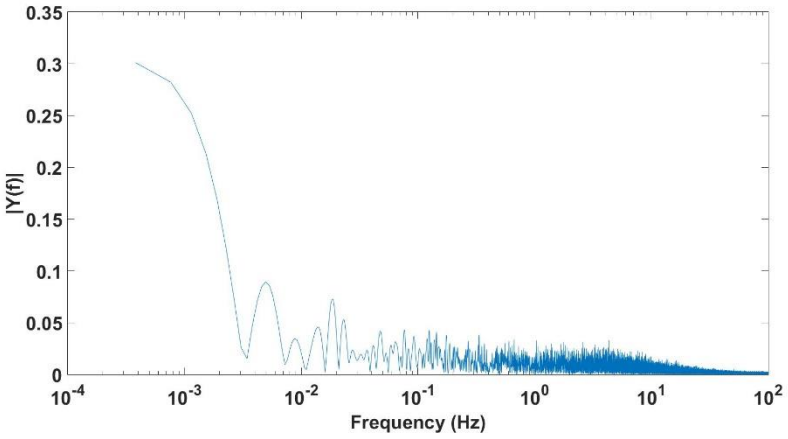

B)

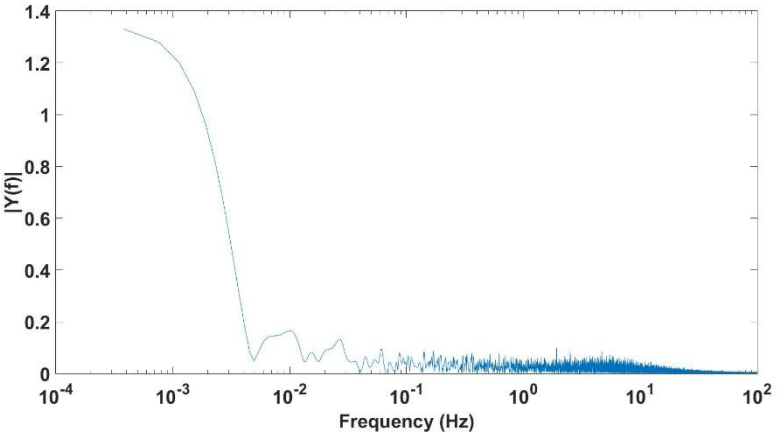

C)

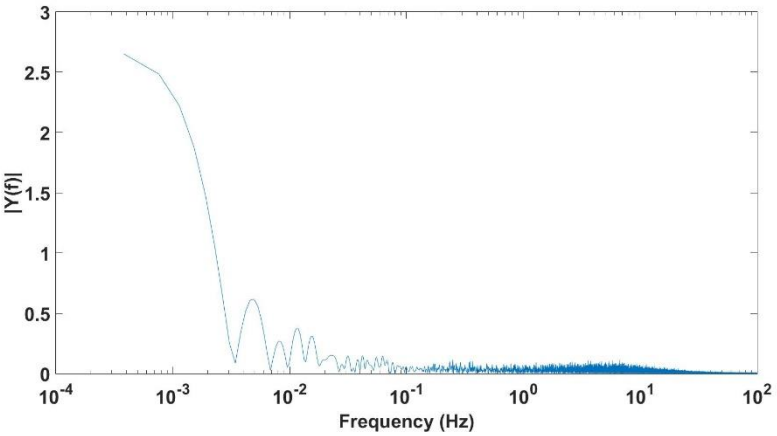

Figure 21: Phase 4: DFT of neuronal network spikes of INEXA with 10% astrocytes. Low (A), medium (B) and high (C) noise responses.

The number of astrocytes in activated state at any given time can be seen from Figure 22. The astrocyte responses to the neuronal network input from medium and high noise seems to cause more calcium signaling than the low noise which has population bursts.

A)

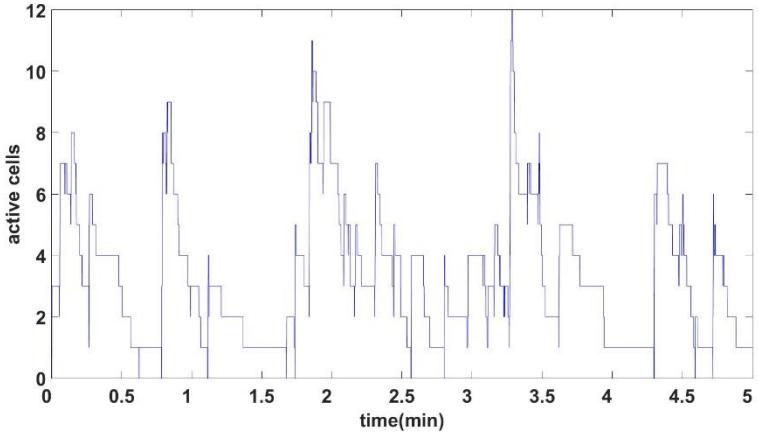

B)

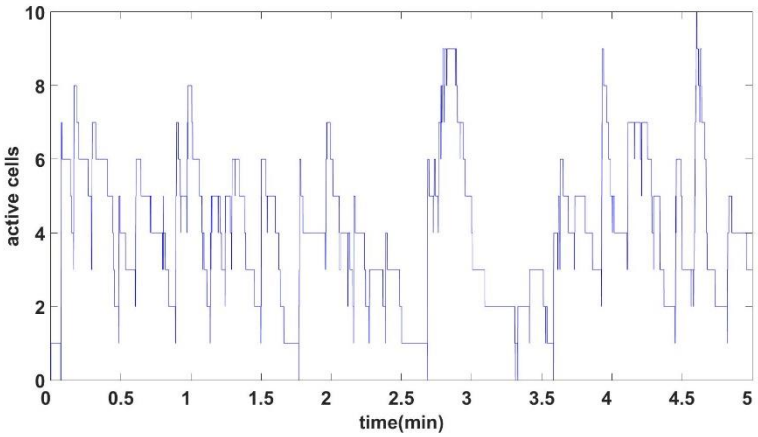

C)

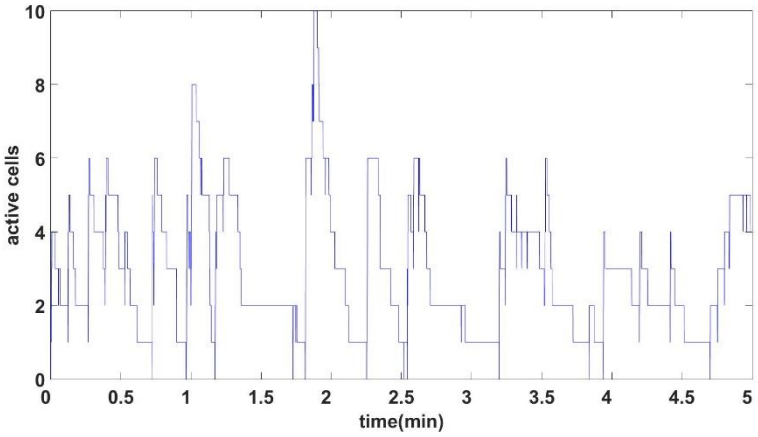

Figure 22: Phase 4: Amount of astrocytes active at any given moment of the simulation. INEXA with 10% astrocytes. Low (A), medium (B) and high (C) noise responses.

4.4.2 20% Astrocytes

In the next set of simulations 63 astrocytes formed the 20% network. 250 neurons and 63 astrocytes totals 313 cells. The network formed can be seen in Figure 23. When compared to 10% astrocytes there are distinct networks forming. However these networks are formed of "islands" of connected astrocytes rather than continuous synctum.

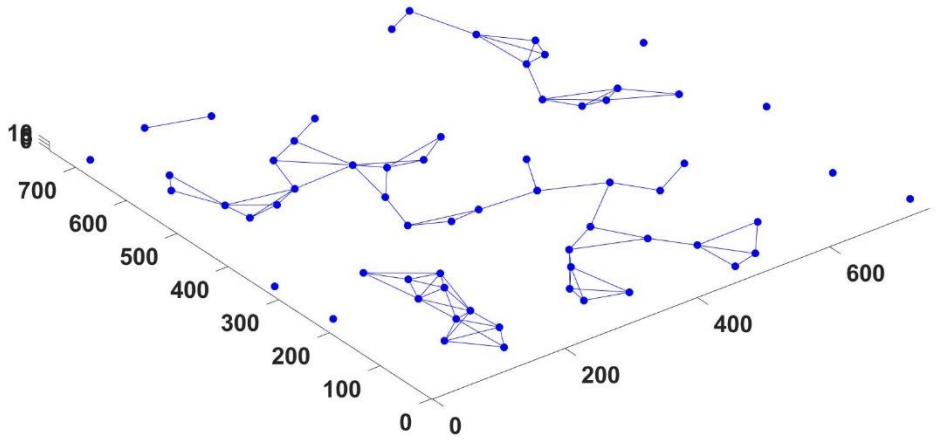

Figure 23: Astrocyte network formed by 63 astrocytes. Culture space is 750µm a side and 10 µm deep.

In the spike trains a clear pattern of population bursts can be seen as a response to low noise (Figure 24 A) and also some population burst like activity in response to medium noise (Figure 24 B) when the astrocytes manage to reduce the network activity enough. In Figure 24 C the effect of added astrocyte amount seems to bring the activity down from the corresponding 10% astrocytes result (Figure 19 C). However it still contains long periods of hyperactivity.

A)

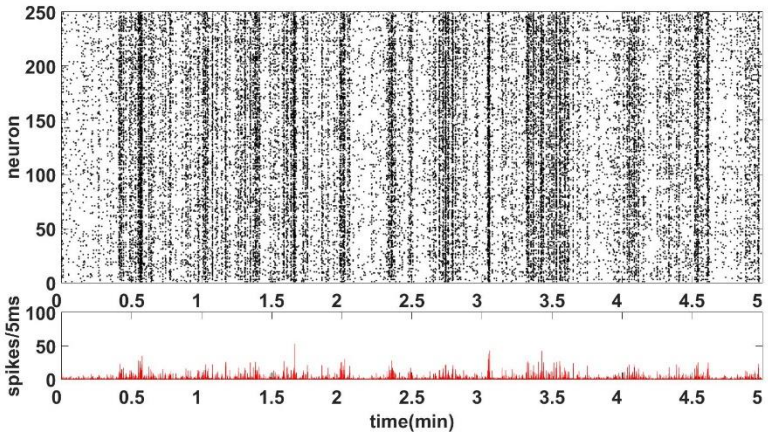

B)

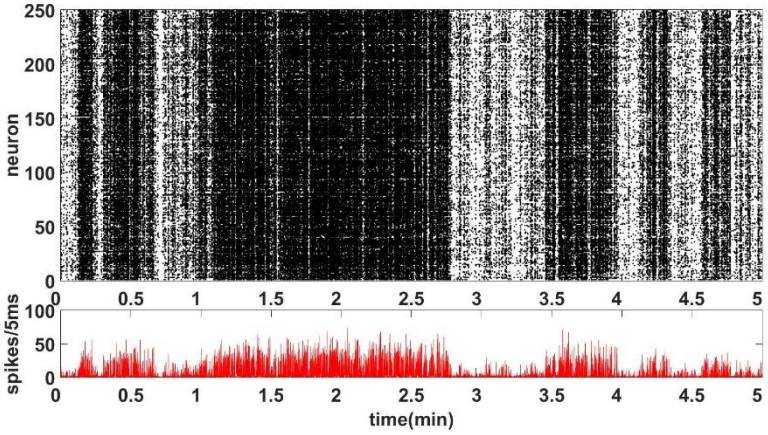

C)

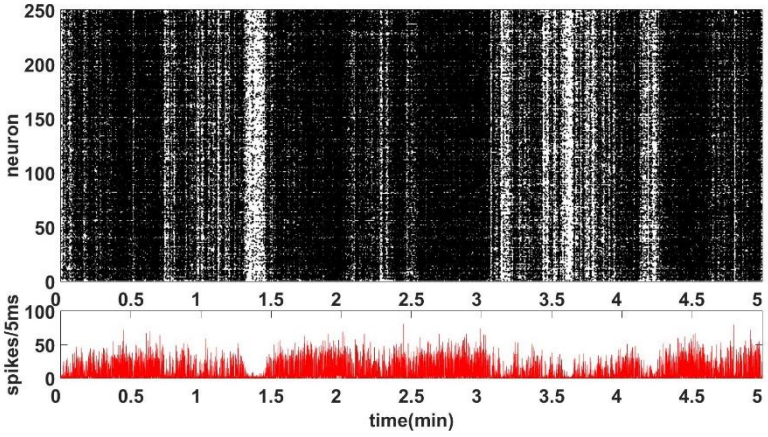

Figure 24: Phase 4. INEXA with 20% astrocytes. Low (A), medium (B) and high (C) noise responses.

The same can be seen in in the DFT results (Figure 25). In response to low noise the high frequency components get more power. However, for medium and high noise responses the DFT distribution is only slightly shifted towards higher frequencies around 10^{-2}.

A)

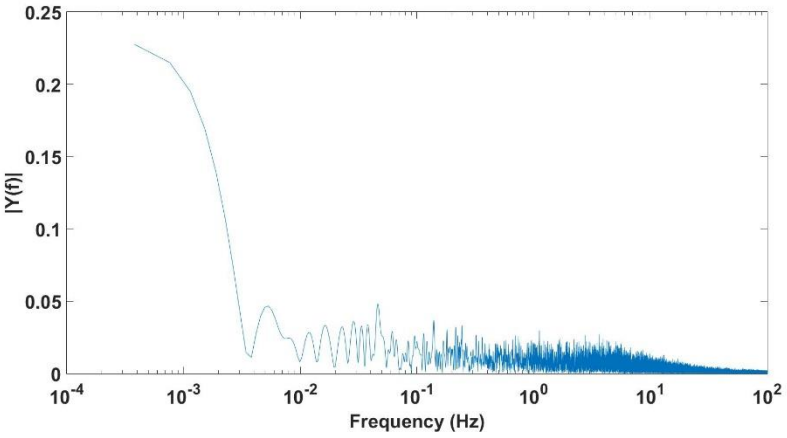

B)

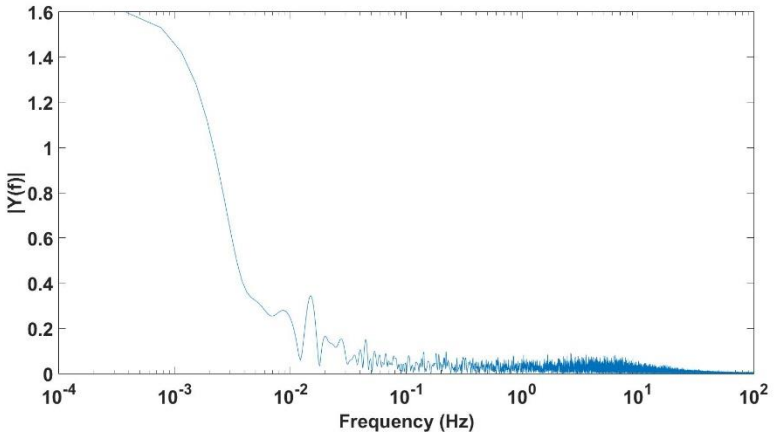

C)

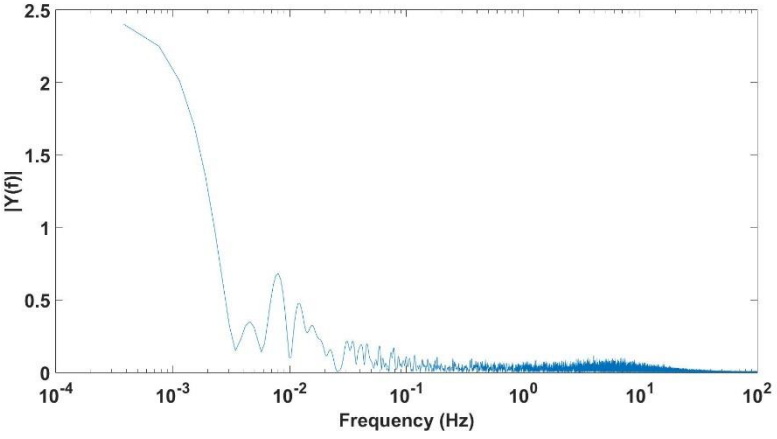

Figure 25: Phase 4: DFT of neuronal network spikes of INEXA with 20% astrocytes. Low (A), medium (B) and high (C) noise responses.

When comparing the activity patterns of 10% and 20% astrocyte responses to different noise levels there is a significant difference. Now the most active network over time seems to be the response to low activity (Figure 26 A) when compared to medium and high (Figure 26 B and C). However, the total number of astrocytes active at high activity stage when there is a high spike is generally lower for response to low noise than for medium and high noise. Estimating from the figures generally 15 astrocytes respond

simultaneously to low noise while 15–25 respond to medium and high noise at one time. Also the activity of the astrocytes seems to be more evenly spread over time in low than in medium and high activity cases.

A)

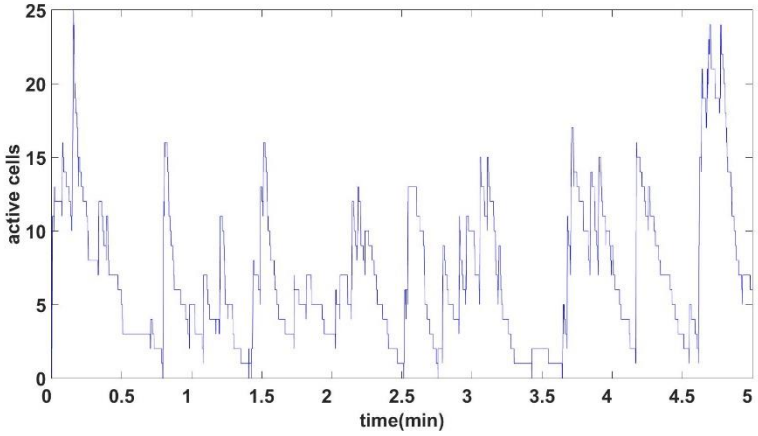

B)

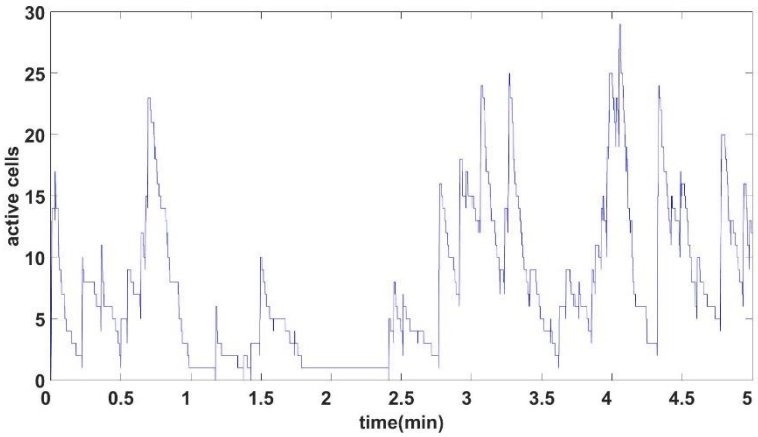

C)

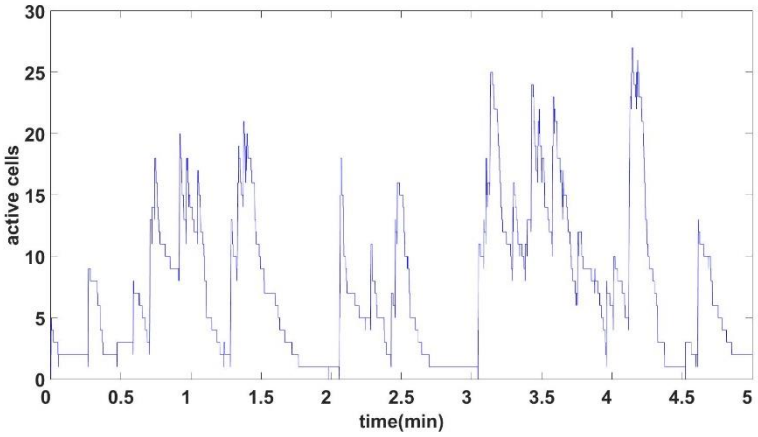

Figure 26: Phase 4: Amount of astrocytes active at any given moment of the simulation. INEXA with 20% astrocytes. Low (A), medium (B) and high (C) noise responses.

4.4.3 30% Astrocytes

In the last simulation of phase 4, 107 astrocytes formed the astrocyte network totaling 30% of the total cell amount. The network formed by the astrocytes can be seen from Figure 27. Now the astrocytes form a single continuous synctum in which the astrocytes are all connected to the same network.

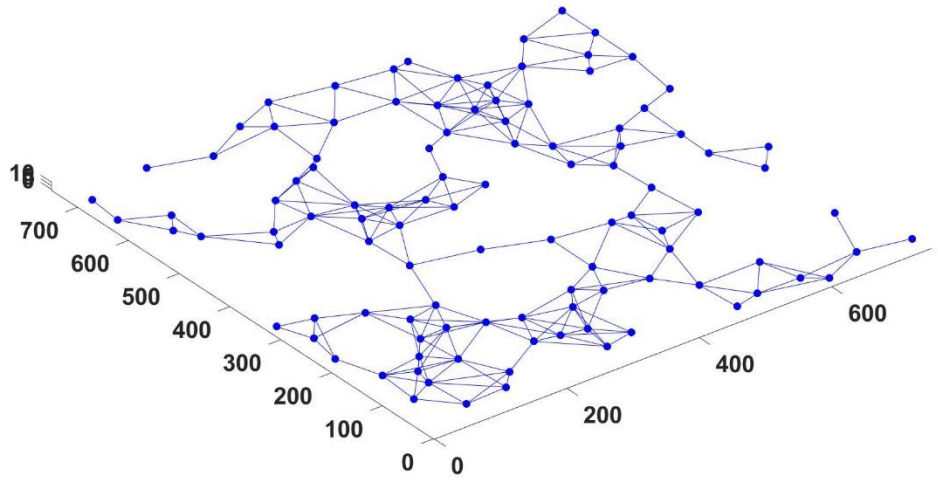

Figure 27: Astrocyte network formed by 107 astrocytes. Culture space is 750µm a side and 10 µm deep.

What is interesting in the neuronal network responses to all noise levels is that they show population burst activity and no hyperactivity (Figure 28).

A)

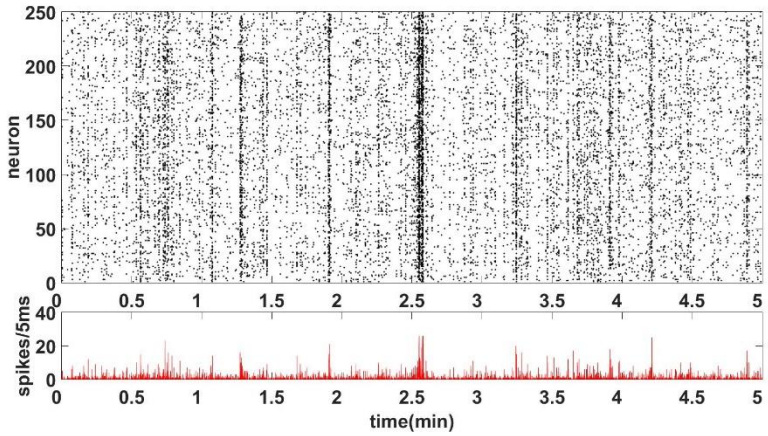

B)

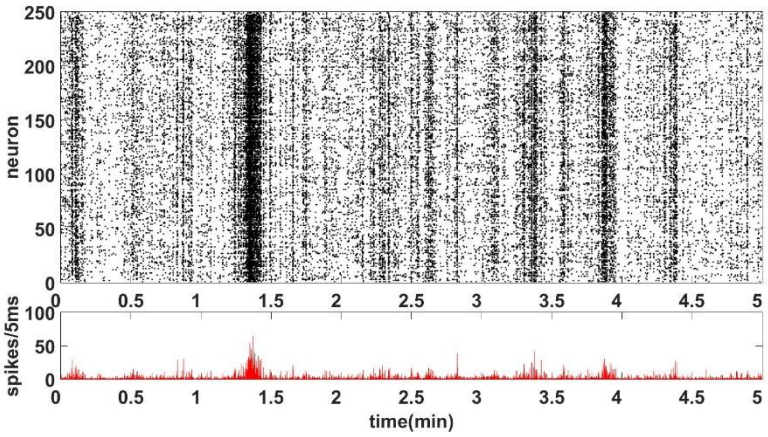

C)

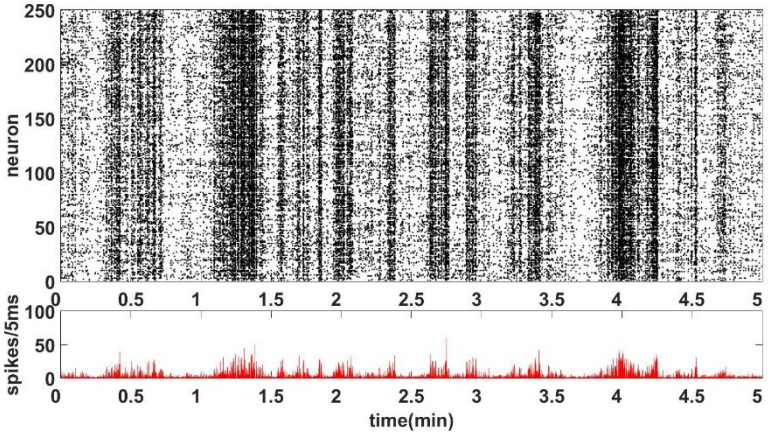

Figure 28: Phase 4. INEXA with 30% astrocytes. Low (A), medium (B) and high (C) noise responses.

The same is clearly visible from the DFT graphs of all the noise level pooled spike counts. All three have significant shift in power to high frequencies (Figure 29).

A)

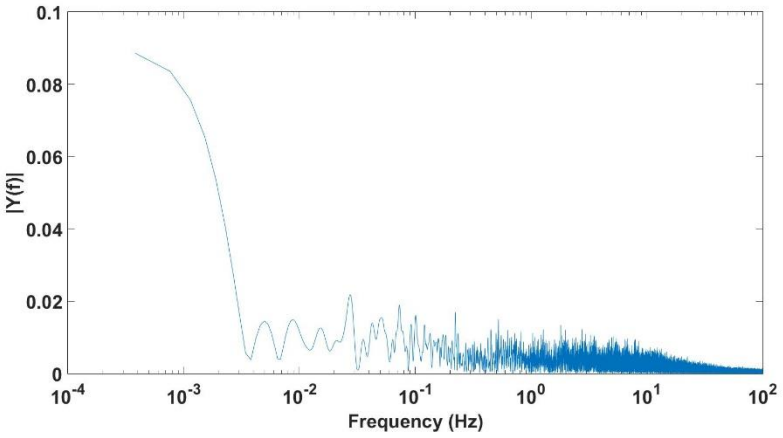

B)

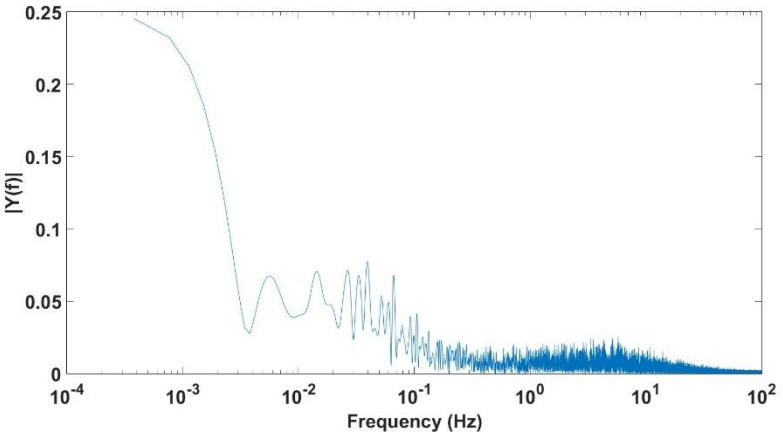

C)

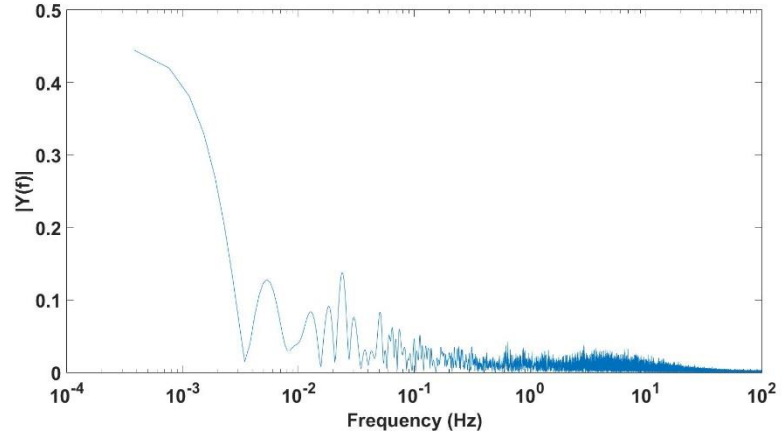

Figure 29: Phase 4: DFT of neuronal network spikes of INEXA with 30% astrocytes. Low (A), medium (B) and high (C) noise responses.

The astrocyte activity in response to different noise levels with 30% astrocytes (Figure 30) show similar behavior as for the 20%. For low noise the activity is more even when going for medium and high activity, the extremes of having fewer or many cells active at one time get to lower and higher cell counts.

A)

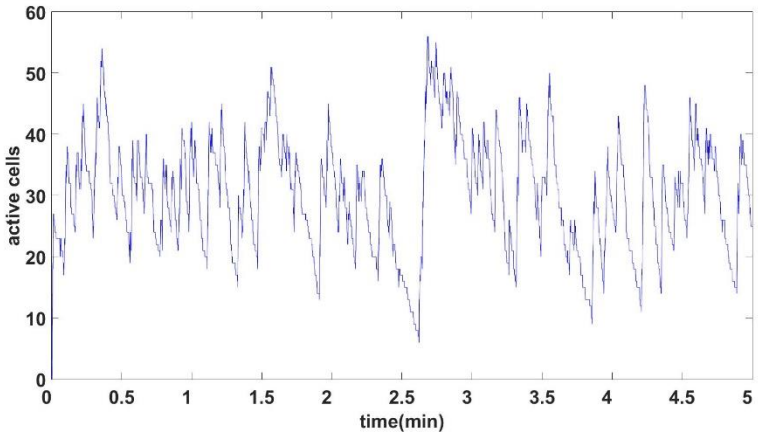

B)

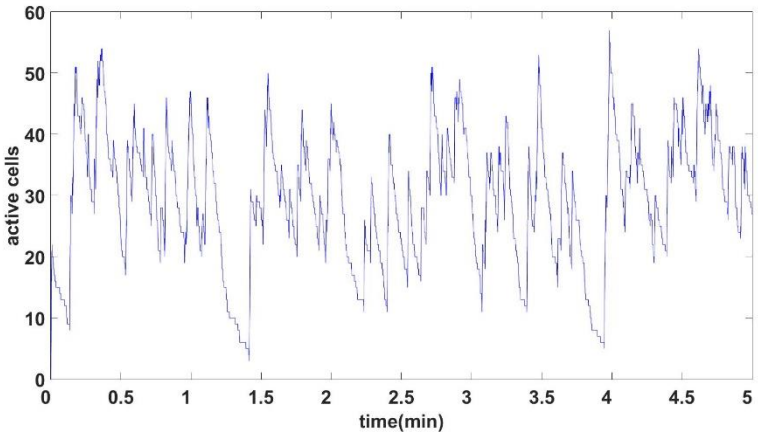

C)

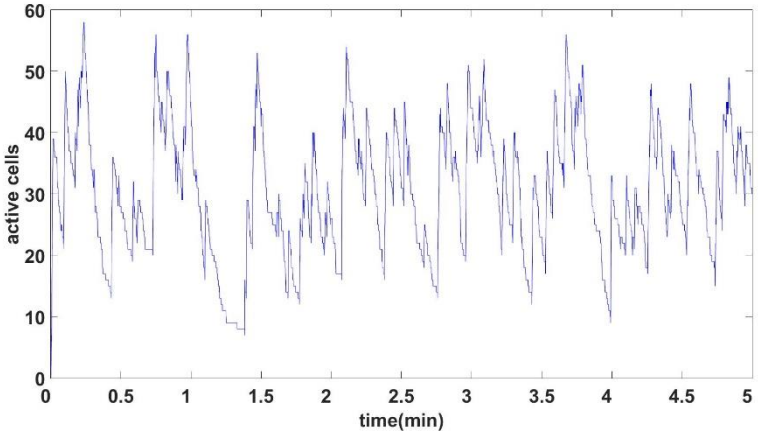

Figure 30: Phase 4: Amount of astrocytes active at any given moment of the simulation. INEXA with 30% astrocytes. Low (A), medium (B) and high (C) noise responses.

5 DISCUSSION

At the beginning we made a hypothesis that the astrocytes should promote bursting behavior in the neuronal network, while restrict hyperactivity. Based on our results this seems plausible. While building the model, a large number of parameters were tested to find sets of parameters that worked together to produce plausible effects. While doing so we were able to see that the effects of each parameter is highly linked to others and as such the model produced results that were not always possible to predict from the way the parameter was changed. Sometimes even small changes had large effects while tuning an important parameter by a lot didn't have much effect. These rise interesting questions about the nature of gliotransmission.

The phase 1 simulations show that the total power of the noise is related to amount of spikes, but the power distribution is similar for all noise levels. When looking relative power distribution it can be seen that more complex patterns have more relative power in the higher frequencies. At phase 2 the neuronal network produces more complex patterns in relation to noise when driven by low noise. However if the noise is high enough the network output power distribution starts to resemble noise again as in medium and high noise responses. Adding presynapse area astrocytes at phase 3 pushes even the low noise response by neuronal network towards noise output. Adding more and more astrocytes at phase 4 has two effects. What the astrocytes seem to do in simulations is to reduce the overall activity based on how much activity there already is, and facilitate communication with burst like patterns at the same time. Especially this can be seen in the Phase 4 30% astrocyte simulations, where all three noise levels produce population bursting activity. It is important to note that while in phase 4 the astrocyte effect is applied only to those synapses, which are controlled by astrocytes, in phase 3 it was applied to all excitatory synapses.

On the other hand the activity of the astrocytes does not reach all the astrocytes at any time. In all the simulations the number of active astrocytes at any given time in most cases stays below half of all the astrocytes. When there are large portions of the astrocytes activated at one go like in the 10% astrocytes response to high noise, there are distinct times between the high activity phases when there is very low activity. This could mean that most of the astrocytes are activated at once due to high input from neurons and all go to refractory period at the same time.

The implications of astrocyte calcium waves would become apparent in this kind of system. Since the astrocyte activity is tied to neuronal activity and astrocytes transmit calcium signal when they get enough input from synapses, the spread of calcium could be interpreted as an attempt to reduce the activity of an overactive network before

exitotoxicity takes place. This can also be seen from a study of spreading depression (Larrosa et al., 2006).

There have been studies that link dysfunction of astrocytes to for example epilepsy and Huntington's disease. (Maragakis & Rothstein, 2006; Seifert et al., 2010; Seifert & Steinhäuser, 2013; Volman et al., 2012). Based on the simulation results showing that the biologically plausible mechanisms for gliotransmission can give astrocytes control over network overall activity as well as signaling patterns. Pathways related to the effects described in the model may be involved.

In the simulations I used a set area for the simulated culture and added astrocytes to create mixtures of cells corresponding to certain percentages of astrocytes. By doing this, the total cell density in the culture was increased by over 28% from 10% astrocytes to 30% astrocytes. In reality the cell cultures with such a difference in cell density would probably have more differences than just connectivity between astrocytes and neurons. However in this work the same neuronal network was used in all the simulations to reduce the probability of the seen changes in the spiking patterns resulting from a change in the neuronal network response due to changed topology. Thus the results seen here should be for the most part be a result of added astrocytes.

The models were combined using knowledge about the biology of the cells and approximations were needed to be done. Thus this model relies on assumptions made in the models and in combining them together with the hypothesis of astrocyte function. When considering the assumptions and approximations made one has to think about variables and parameters used to build the model. The INEX has already been used for simulation of neuronal networks and it has proven to work for simulations of MEA plate culture spiking patterns. The next part to be added was the tripartite synapse. The synapse was scaled so that it uses the INEX synaptic strengths and takes out the synapse from the black box simulation. The INEX synapse strength of one representing full release was scaled so that the full release corresponds to the higher limit of the boundaries. This allowed us to scale the memory containing Tsodyks-Markram synapse independent of a hard set limiter of one for full release. The addition of the presynapse simulator interface was done at the same time. Since the simulation uses relatively large networks the dynamics had to be kept as simple as possible. For example 250 neurons having 25% connectivity meant roughly 15000 synapses to be simulated.

The alpha parameter introduced by De Pittá et al. is an important for the control of the network. If we consider the effects described by De Pittá et al. for paired pulse facilitation and depression we can already see that the network behavior is highly related to the alpha parameter together with the gliotransmission by astrocytes. The value of alpha determines the level of synaptic strength towards which the gliotransmission shifts synaptic strengths. From the results by De Pittá et al. (De Pittà et al., 2011), it can be seen that the alpha parameter can cause a synapse to change from paired pulse facilitation (PPF) to paired

pulse depression (PPD) and vice versa depending on the alpha parameter and gliotransmitter effect. That means that a synapse with low initial RR has PPF and when it gets glutamate and alpha is high it turns into PPD synapse. A synapse with high initial RR has PPD and turns into PPF. We used a value that increases synaptic strength for most of the synapses according to the presynapse response to glutamate. However since some of the synapses had their initial strengths higher than the alpha some of the synapses actually got depressed by gliotransmission.

Increased releases at synapses at high activity induces more activity in the network as can be seen when comparing phase 2 and 3 simulations. This would mean that a network with high enough activity can't get out of the high activity mode as seen in the results of phase 3 simulations. If the only way for the network to leave the high activity state was by stopping the activity for a moment it might not be able to. In such a case the network could lock into high activity "epileptic" mode. Eventually it would result in excitotoxicity.

What was suggested as a solution is backed up by experimental findings. Since the high activity needs to be calmed down and the astrocytes already monitor most of the synapses, it would be logical if they could inhibit the network activity in this case. If the astrocytes release GABA during full cell calcium signaling, and glutamate and ATP at a much lower concentration, that would also provide a means for astrocytic inhibition during overactive phase. GABA is shown to be a key transmitter for tonic inhibition by astrocytes (Yoon et al., 2011). However, not all astrocytes in different brain areas contained GABA. The effect of astrocyte released GABA causing synchronous inhibition at postsynaptic neurons has been suggested also by others (Angulo et al., 2008; Kozlov et al., 2006; Liu, Schaffner, Chang, Maric, & Barker, 2000).

As was mentioned, the model has to be built with relatively simple components to keep it computationally as light as possible. As such many of the parameters have been deduced from other papers and some have been set by testing the model and with educated guess. However, the the amount of parameters in the model has considerably increased from the original INEX. The parameters at INEX are phenomenological. This means that anything we build on top of it will be phenomenological as well. By adding Tsodyks-Markram presynapse model we introduced another phenomena into the INEX, which was the memory at a single synapse level. The parameters for these were adapted from paper by De Pittá (2011). The INEX parameters were found using brute force to find sets of parameters that produced results in reasonable ranges. The near synapse area astrocyte simulator has the calcium and IP3 variables. These are not accurate descriptions of what truly happens in astrocytes and as such the presynapse area astrocyte values are educated guesses. Thus the variables describing astrocyte calcium and IP3 are just numerical. The UAR model uses the parameters described in the supplementary of the paper by Lallouette et al. (Lallouette et al., 2014). The GABA inhibition strength was an educated guess based on trial and error tuned so that the astrocyte don't kill off the neurons signaling

completely, but greatly reduced the probability of it spiking. The building of neuron and astrocyte networks was done by selecting an area that would be reasonable for a cultured network on a microelectrode array. Then the amount of astrocytes was selected. 250 neurons were found to be reasonably fast to compute since many runs were needed to optimize parameters. The network building values for neurons were selected so that they formed a network with roughly 25% connectivity. Astrocytes were set to be at least 30µm apart. The simulation does not take into account the exact micro domains (Bushong et al., 2002) occupied by astrocytes but assumes that the shape of the astrocytes allows them to occupy spaces that are vaguely around the cell soma, which is located around the coordinates given to the cell. As such the astrocytes are connected if they are within 100µm of each other. It is possible that two astrocytes are connected even if there is an astrocyte between them. In these cases the astrocyte domains are assumed to be in touch so that there is a physical contact between the two astrocytes going around the one in the middle. Similarly because the domains are slightly vague the astrocyte-neuron connections are possible to form if the distance between the cells is 70µm or less. This vague definition of astrocyte occupied domain also means that there is no need to set a hard limiter for how close a neuron and an astrocyte can be of each other.

When comparing with the other models one thing in common with all the simulations seems to be some kind of switch between two different firing states of the neurons. The INEXA seems to produce such effect in whole network level. The model seems to work well when taking into account all the approximations that needed to be made. It would seem plausible that if these mechanisms are present in real neuron-astrocyte networks, they could have a part to play in epileptic seizures due to their ability to control the whole network activity. If the balance between spike inducing glutamate dynamics and network balancing inhibitory pathway is disturbed it might result in increased activity of the neuronal network.

The model as it is works for studying the effects shown. However it would be also possible to add inhibitory neuron control to astrocytes as well as diffusion of transmitters in culture space. For example the diffusion of ATP and its effect in astrocyte calcium signaling could be studied this way. Also the hydrolysis of the ATP to adenosine and its time delayed effect could be studied in the culture. Eventually this could perhaps be used to study what happens to the neuronal signaling when the cerebrospinal fluid washes the tissue of excess transmitters and molecules in our sleep.

The next step in developing the model should be to make a fit for parameters to match biological data. After that the model could have some predictive power for scenarios that have not yet been studied *in vitro*.

6 SUMMARY AND CONCLUSIONS

Astrocytes are a type of glia-cells that are ideally positioned for local information processing in the brain. In this work we tried to create a simulation scheme that would describe the effect of astrocyte network to neuronal network. For this purpose three existing models were used. I built a model using the best features of all the three existing models. The model was built and tested on Matlab. Each phenomenon was separately tested and the outputs of each phase were run step by step. To ensure that the simulations run smoothly even with massive amounts of synapses, the code was built so that it uses as much matrixes as possible in the calculations. Even so the simulator is computationally heavy and the runtime increases exponentially when adding more neurons and astrocytes. The parameters were optimized based on literature and trial and error in finding parameters that produced a system where the phenomena described in literature could be seen. Then each of those parameters were adjusted to fit together.

By combining INEX by Kerstin Lenk (Lenk, 2011), Presynapse simulator by De Pittá et al. (De Pittà et al., 2011) using Tsodyks-Markram synapse model (Tsodyks & Markram, 1997) and astrocyte calcium signaling model UAR by Lallouette et al. (Lallouette et al., 2014) in a biologically reasonable way, the INEXA astrocyte-neuron network simulator was created.

Eighteen simulation runs were made with different settings to see the effect of added astrocytes to the network behavior. This was done in four phases, where first phase consisted of simulations with only the noise produced by different basic activities of the neurons. In the second phase neuronal network response with Tsodyks-Markram presynapses was run to see the neuronal network response to the noise. In the third phase presynapse area astrocytes were added. The simulations showed that the astrocytes with only increasing effect just increase the network activity. In phase 4 full INEXA astrocyte model was applied with different amounts of astrocytes. The results show that when there are enough astrocytes they reduce the overall activity and start to promote communication by bursting.

In this thesis for the first time astrocyte-neuron networks were modeled at this level. Astrocytes with biologically plausible effects were modeled together with neuronal network simulator INEX to find out what kind of effect astrocytes could have to neuronal network behavior. The hypothesis was that the astrocytes should promote bursting behavior in the neuronal network, while restricting hyperactivity. This seems plausible based on the simulation results. If astrocytes communicate with the neurons this way it is no surprise that dysfunction in astrocyte function could be related to diseases like epilepsy and Huntington’s. This is the first model to combine all the components in this scale into a computational framework.

REFERENCES

Abbott, N. J., Patabendige, A. A. K., Dolman, D. E. M., Yusof, S. R., & Begley, D. J. (2010). Structure and function of the blood-brain barrier. *Neurobiology of Disease*, *37*(1), 13–25.

Alberts, B., Bray, D., Karen, H., Johnson, A., Lewis, J., Raff, M., … Walter, P. (2009). *Essential Cell Biology* (Third Edit). New York: Garland Science.

Amiri, M., Bahrami, F., & Janahmadi, M. (2012). Functional contributions of astrocytes in synchronization of a neuronal network model. *Journal of Theoretical Biology*, *292*, 60–70.

Angulo, M. C., Le Meur, K., Kozlov, A. S., Charpak, S., & Audinat, E. (2008). GABA, a forgotten gliotransmitter. *Progress in Neurobiology*, *86*(3), 297–303.

Bear, M., Connors, B., & Paradiso, M. (2007). *Neuroscience, Exploring the brain* (Third Edit). Lippincott Williams & Wilkins.

Bonansco, C., Couve, A., Perea, G., Ferradas, C. Á., Roncagliolo, M., & Fuenzalida, M. (2011). Glutamate released spontaneously from astrocytes sets the threshold for synaptic plasticity. *The European Journal of Neuroscience*, *33*(8), 1483–92.

Bushong, E. A., Martone, M. E., Jones, Y. Z., & Ellisman, M. H. (2002). Protoplasmic Astrocytes in CA1 Stratum Radiatum Occupy Separate Anatomical Domains. *J. Neurosci.*, *22*(1), 183–192. Retrieved from

Collins, C. E., Airey, D. C., Young, N. A., Leitch, D. B., & Kaas, J. H. (2010). Neuron densities vary across and within cortical areas in primates. *Proceedings of the National Academy of Sciences of the United States of America*, *107*(36), 15927–32.

De Pittà, M., Goldberg, M., Volman, V., Berry, H., & Ben-Jacob, E. (2009). Glutamate regulation of calcium and IP3 oscillating and pulsating dynamics in astrocytes. *Journal of Biological Physics*, *35*(4), 383–411.

De Pittà, M., Volman, V., Berry, H., & Ben-Jacob, E. (2011). A tale of two stories: astrocyte regulation of synaptic depression and facilitation. *PLoS Computational Biology*, *7*(12), e1002293.

De Pittà, M., Volman, V., Berry, H., Parpura, V., Volterra, A., & Ben-Jacob, E. (2012). Computational quest for understanding the role of astrocyte signaling in synaptic transmission and plasticity. *Frontiers in Computational Neuroscience*, *6*, 98.

Feldman, R. P., & Goodrich, J. T. (1999). The Edwin Smith Surgical Papyrus. *Child's Nervous System*, *15*(6-7), 281–284.

Fellin, T. (2009). Communication between neurons and astrocytes: relevance to the modulation of synaptic and network activity. *Journal of Neurochemistry*, *108*(3), 533–44.

Földes-Papp, Z., Demel, U., & Tilz, G. P. (2003). Laser scanning confocal fluorescence microscopy: an overview. *International Immunopharmacology*, *3*(13-14), 1715–29.

Golovina, V. A. (1997). Spatially and Functionally Distinct Ca2+ Stores in Sarcoplasmic and Endoplasmic Reticulum. *Science*, *275*(5306), 1643–1648.

Gordleeva, S. Y., Stasenko, S. V, Semyanov, A. V, Dityatev, A. E., & Kazantsev, V. B. (2012). Bi-directional astrocytic regulation of neuronal activity within a network. *Frontiers in Computational Neuroscience*, *6*, 92.

Halassa, M. M., Fellin, T., Takano, H., Dong, J.-H., & Haydon, P. G. (2007). Synaptic islands defined by the territory of a single astrocyte. *The Journal of Neuroscience : The Official Journal of the Society for Neuroscience*, *27*(24), 6473–7.

Heikkilä, T. J., Ylä-Outinen, L., Tanskanen, J. M. a, Lappalainen, R. S., Skottman, H., Suuronen, R., … Narkilahti, S. (2009). Human embryonic stem cell-derived neuronal cells form spontaneously active neuronal networks in vitro. *Experimental Neurology*, *218*(1), 109–116.

Hines, D. J., & Haydon, P. G. (2014). Astrocytic adenosine: from synapses to psychiatric disorders. *Philosophical Transactions of the Royal Society of London. Series B, Biological Sciences*, *369*(1654), 20130594–.

Hirase, H., Iwai, Y., Takata, N., Shinohara, Y., & Mishima, T. (2014). Volume transmission signalling via astrocytes. *Philosophical Transactions of the Royal Society of London. Series B, Biological Sciences*, *369*(1654), 20130604–.

Johnstone, A. F. M., Gross, G. W., Weiss, D. G., Schroeder, O. H.-U., Gramowski, A., & Shafer, T. J. (2010). Microelectrode arrays: a physiologically based neurotoxicity testing platform for the 21st century. *NeuroToxicology*, *31*(4), 331–350.

Jourdain, P., Bergersen, L. H., Bhaukaurally, K., Bezzi, P., Santello, M., Domercq, M., … Volterra, A. (2007). Glutamate exocytosis from astrocytes controls synaptic strength. *Nature Neuroscience*, *10*(3), 331–9.

Jueptner, M., & Weiller, C. (1995). Review: Does Measurement of Regional Cerebral Blood Flow Reflect Synaptic Activity?—Implications for PET and fMRI. *NeuroImage*, *2*(2), 148–156.

Kettenmann, H., & Verkhratsky, A. (2008). Neuroglia: the 150 years after. *Trends in Neurosciences*, *31*(12), 653–9.

Kiernan, john A. (2005). *BARR's The Human Nervous System* (Ninth). Philadelphia: Lippincott Williams & Wilkins.

Kozlov, A. S., Angulo, M. C., Audinat, E., & Charpak, S. (2006). Target cell-specific modulation of neuronal activity by astrocytes. *Proceedings of the National Academy of Sciences of the United States of America*, *103*(26), 10058–63.

Lallouette, J., De Pittà, M., Ben-Jacob, E., & Berry, H. (2014). Sparse short-distance connections enhance calcium wave propagation in a 3D model of astrocyte networks. *Frontiers in Computational Neuroscience*, *8*, 45.

Lalo, U., Palygin, O., Rasooli-Nejad, S., Andrew, J., Haydon, P. G., & Pankratov, Y. (2014). Exocytosis of ATP from astrocytes modulates phasic and tonic inhibition in the neocortex. *PLoS Biology*, *12*(1), e1001747.

Larrosa, B., Pastor, J., López-Aguado, L., & Herreras, O. (2006). A role for glutamate and glia in the fast network oscillations preceding spreading depression. *Neuroscience*, *141*(2), 1057–68.

Lenk, K. (2011). A Simple Phenomenological Neuronal Model with Inhibitory and Excitatory Synapses. In C. M. Travieso-González & J. B. Alonso-Hernández (Eds.), *Advances in Nonlinear Speech Processing* (pp. 232–238).

Lenk, K., & Priwitzer, B. (2011). Frontiers: Large-scale modeling for simulating multi-electrode array neurochip recordings. In *BC11 : Computational Neuroscience & Neurotechnology Bernstein Conference & Neurex Annual Meeting*.

Liu, Q.-Y., Schaffner, A. E., Chang, Y. H., Maric, D., & Barker, J. L. (2000). Persistent Activation of GABAA Receptor/Cl- Channels by Astrocyte-Derived GABA in Cultured Embryonic Rat Hippocampal Neurons. *J Neurophysiol*, *84*(3), 1392–1403.

Llinás, R., Steinberg, I. Z., & Walton, K. (1981). Relationship between presynaptic calcium current and postsynaptic potential in squid giant synapse. *Biophysical Journal*, *33*(3), 323–51.

López-Hidalgo, M., & Schummers, J. (2014). Cortical maps: a role for astrocytes? *Current Opinion in Neurobiology*, *24*(1), 176–89.

Maragakis, N. J., & Rothstein, J. D. (2006). Mechanisms of Disease: astrocytes in neurodegenerative disease. *Nature Clinical Practice. Neurology*, *2*(12), 679–89.

Matthews, G. G. (2007). Cellular Physiology of Nerve and Muscle,. *Cellular Physiology of Nerve and Muscle*, 1–11.

McIver, S. ., Faideau, M., & Haydon, P. G. (2013). Astrocyte-Neuron Communications. In *Neural-Immune Interactions in Brain Function and Alcohol Related Disorders* (p. 587).

Min, R., Santello, M., & Nevian, T. (2012). The computational power of astrocyte mediated synaptic plasticity. *Frontiers in Computational Neuroscience*, *6*, 93.

Papouin, T., & Oliet, S. H. R. (2014). Organization, control and function of extrasynaptic NMDA receptors. *Philosophical Transactions of the Royal Society of London. Series B, Biological Sciences*, *369*(1654), 20130601–.

Paredes, R. M., Etzler, J. C., Watts, L. T., Zheng, W., & Lechleiter, J. D. (2008). Chemical calcium indicators. *Methods (San Diego, Calif.)*, *46*(3), 143–51.

Parri, H. R., Gould, T. M., & Crunelli, V. (2001). Spontaneous astrocytic Ca2+ oscillations in situ drive NMDAR-mediated neuronal excitation. *Nature Neuroscience*, *4*(8), 803–12.

Perea, G., & Araque, A. (2005). Glial calcium signaling and neuron-glia communication. *Cell Calcium*, *38*(3-4), 375–82.

Perea, G., & Araque, A. (2007). Astrocytes potentiate transmitter release at single hippocampal synapses. *Science (New York, N.Y.)*, *317*(5841), 1083–6.

Perea, G., Navarrete, M., & Araque, A. (2009). Tripartite synapses: astrocytes process and control synaptic information. *Trends in Neurosciences*, *32*(8), 421–31.

Polikov, V. S., Tresco, P. A., & Reichert, W. M. (2005). Response of brain tissue to chronically implanted neural electrodes. *Journal of Neuroscience Methods*, *148*(1), 1–18.

Porter, J. T., & McCarthy, K. D. (1996). Hippocampal Astrocytes In Situ Respond to Glutamate Released from Synaptic Terminals. *J. Neurosci.*, *16*(16), 5073–5081.

Porto-Pazos, A. B., Veiguela, N., Mesejo, P., Navarrete, M., Alvarellos, A., Ibáñez, O., … Araque, A. (2011). Artificial astrocytes improve neural network performance. *PloS One*, *6*(4), e19109.

Sahlender, D. A., Savtchouk, I., & Volterra, A. (2014). What do we know about gliotransmitter release from astrocytes? *Philosophical Transactions of the Royal Society of London. Series B, Biological Sciences*, *369*(1654), 20130592–.

Seifert, G., Carmignoto, G., & Steinhäuser, C. (2010). Astrocyte dysfunction in epilepsy. *Brain Research Reviews*, *63*(1-2), 212–21.

Seifert, G., & Steinhäuser, C. (2013). Neuron-astrocyte signaling and epilepsy. *Experimental Neurology*, *244*, 4–10.

Sofroniew, M. V. (2005). Reactive astrocytes in neural repair and protection. *The Neuroscientist : A Review Journal Bringing Neurobiology, Neurology and Psychiatry*, *11*(5), 400–7.

Swanson, R. A., & Graham, S. H. (1994). Fluorocitrate and fluoroacetate effects on astrocyte metabolism in vitro. *Brain Research*, *664*(1-2), 94–100. Retrieved from

Takano, T., Tian, G.-F., Peng, W., Lou, N., Libionka, W., Han, X., & Nedergaard, M. (2006). Astrocyte-mediated control of cerebral blood flow. *Nature Neuroscience*, *9*(2), 260–7.

Tsodyks, M. V., & Markram, H. (1997). The neural code between neocortical pyramidal neurons depends on neurotransmitter release probability. *Proceedings of the National Academy of Sciences*, *94*(2), 719–723.

Wallach, G., Lallouette, J., Herzog, N., De Pittà, M., Ben Jacob, E., Berry, H., & Hanein, Y. (2014). Glutamate mediated astrocytic filtering of neuronal activity. *PLoS Computational Biology*, *10*(12), e1003964.

Veletić, M., Mesiti, F., Floor, P. A., & Balasingham, I. (2015). Stochastic Modeling the Tripartite Synapse and Applications.

Winship, I. R., Plaa, N., & Murphy, T. H. (2007). Rapid astrocyte calcium signals correlate with neuronal activity and onset of the hemodynamic response in vivo. *The Journal of Neuroscience : The Official Journal of the Society for Neuroscience*, *27*(23), 6268–72.

Volman, V., Bazhenov, M., & Sejnowski, T. J. (2012). Computational models of neuron-astrocyte interaction in epilepsy. *Frontiers in Computational Neuroscience*, *6*, 58.

Yoon, B.-E., Jo, S., Woo, J., Lee, J.-H., Kim, T., Kim, D., & Lee, C. J. (2011). The amount of astrocytic GABA positively correlates with the degree of tonic inhibition in hippocampal CA1 and cerebellum. *Molecular Brain*, *4*(1), 42.

APPENDIX 1

Parameter	Value	Name
Boundary c	0.01, 0.02, 0.03	Upper boundary
Boundary y^{+}_{ji}	0.7	Upper boundary
Boundary y^{-}_{ji}	-0.7	Upper boundary
LengthST	300 000	Length of the simulation in ms
regenR	0.02	Percentage of transmitters regenerated per time slot
regenCa	0.998	Percentage of calcium left at the presynapse after each millisecond
α	0.7	alpha
g_{dg}	0.999923	Percentage of glutamate left at the presynaptic receptors after each millisecond
g_r	0.3	Percentage of receptors not having gliotransmitters bound to it getting bound at astrocyte release
Ca_{th}	0.1	Calcium threshold for gliotransmitter release
acc	0.05	Accumulation rate between IP3 and Ca
IP_{3dg}	0.85873	Percentage of IP_3 left after each millisecond at the near synapse areas.
Astrocytes	28,63,107	Number of astrocytes at each simulation.
M	1000	Multiplier between astrocyte near synapse and whole astrocyte self-induced IP_3 flux.
Connection distance	100	Maximum distance between two connected astrocytes in µm
A_{time}	1500	Parameter used to determine probability of stage change
R_{time}	7000	Parameter used to determine probability of stage change
U_{time}	5000	Parameter used to determine probability of stage change
Slope	0.02	Increase in required flux to activate an astrocyte for each connection it has
Intersect	0.205	Minimum flux needed to activate an astrocyte
y_{GABA}	-0.01	Inhibition applied by astrocytes in GABA signaling through each controlled synapse
Culture area	[750 750 10]	µm
Minimum neuron distance	10	µm
Minimum astrocyte distance	30	µm
Neuro STD	200	(µm) standard deviation of neuronal connections
Astrocyte STD	150	(µm) standard deviation of astrocyte-neuron connections without limiter
Max astrocyte reach distance	70	(µm) limiter cutting the gaussian standard deviation connection probability set by standard deviation

APPENDIX 2

Merope: General Information

- Appr. 1500 CPU cores, total memory 4.3TB RAM, raw disk 200TB.
- GPU/CUDA nodes with two NVIDIA M2090 GPU cards (each card with 6GB RAM).
- A *bigmem* server with 512GB RAM and 32 CPU cores.
- Infiniband network (QDR/FDR).
- Scientific Linux release 6.5 (64bit) operating system.
- SLURM batch job scheduler.

The **"parallel" partition** contains compute nodes with 48GB of memory and max runtime is 1 day. Each of the nodes contains two Intel X5660 processors (192 CPU cores). Nodes should preferable be reserved completely for a single job allocation, such as 24, 36, 48, (and so on) CPU cores at a time.

The **"bigmem" partition** contains one compute node with 512 GB of memory and four eight-core Intel X7550 processor (32 CPU cores).

Matlab R2013b